2011-01-01

Experimental Investigation of Magnesium/ Regolith Combustion for In-Situ Production of Materials on the Moon

Christopher White
University of Texas at El Paso, cwhite2@miners.utep.edu

EXPERIMENTAL INVESTIGATION OF MAGNESIUM/REGOLITH COMBUSTION FOR IN-SITU PRODUCTION OF MATERIALS ON THE MOON

CHRISTOPHER WHITE

Department of Mechanical Engineering

APPROVED:

Evgeny Shafirovich, Ph.D., Chair

Cesar Carrasco, Ph.D.

Yirong Lin, Ph.D.

Benjamin C. Flores, Ph.D.
Acting Dean of the Graduate School

EXPERIMENTAL INVESTIGATION OF MAGNESIUM/REGOLITH COMBUSTION FOR IN-SITU PRODUCTION OF MATERIALS ON THE MOON

by

CHRISTOPHER WHITE

THESIS

Presented to the Faculty of the Graduate School of

The University of Texas at El Paso

in Partial Fulfillment

of the Requirements

for the Degree of

MASTER OF SCIENCE

Department of Mechanical Engineering

THE UNIVERSITY OF TEXAS AT EL PASO

December 2011

Acknowledgements

I would first like to thank my advisor, Dr. Evgeny Shafirovich, for involving me in his research, as well as Dr. Ahsan Choudhuri, director of UTEP's Center for Space Exploration Technology and Research (cSETR) and chair of the Department of Mechanical Engineering, for his financial and organizational support. Nate Robinson, associate director for cSETR, deserves a great deal of thanks for his support and encouragement. He has worked hard to keep the labs safe and running smoothly during a time of transition for what has become a very specialized research center. I'd also like to thank Dr. David Borrok for generously providing us with JSC-1A; David Brown, for his practical advice and assistance on measurement and microscopy techniques; Dr. Thomas Gill, for his assistance in providing laser diffraction data; Dr. John McClure, Dr. Chintalapalle Ramana, and my brother, Stephen White, for their help in attaining and evaluating XRD data; Mohammed Noor-A-Alam, for his help in attaining XRD, SEM and EDS results; Dr. Cesar Carrasco and Dr. Yirong Lin, for hearing my oral defense; and finally, my fellow team members Francisco Alvarez, Mario Rubio, Armando Delgado, Jorge Frias, and Ashvin Narayana Swamy for their help in just about everything. This has truly been a team effort, and I'm very lucky to have worked with all of them.

Last but certainly not least, I'd like to extend my deepest thanks to the NASA Office of Education for both their support and advice, the Reduced Gravity Flight Office for their astounding work and guidance before and during flight week, and Michelle Jones of Johnson Space Center, who was of great help in preparing me and my team for our reduced-gravity flight experiments.

Abstract

Future settlements on the Moon will require that strong, cost-effective structural materials be developed in whole or in part from locally available resources. Such materials can be created *in-situ* from the lunar regolith using self-propagating high-temperature synthesis (SHS). By mixing the lunar regolith with metal additives, such as aluminum or magnesium, a combustible mixture is formed which, when ignited, can reach temperatures high enough to allow combustion to be self-sustaining, sintering the lunar regolith without further energy input and without the need for atmospheric oxygen. The resulting products may be strong enough for some structural applications, such as radiation shielding, high-temperature thermal insulation, launch pads, and thermal wadis. Thermodynamic calculations and experiments were successfully performed using mixtures of lunar simulant JSC-1A and magnesium. The present investigation is focused on the predictions of thermodynamic calculations for magnesium mixtures with an emphasis on predicted compositions, the effects of milling on simulant characteristics and propagation of the combustion wave, the effect of gravity upon combustion products, the minimization of magnesium content in the reaction, and unstable combustion phenomena encountered during experiments.

Table of Contents

List of Tables

List of Figures

1. Introduction

The cost of sending structural materials into space, let alone successfully deploying them onto the lunar surface, is prohibitive. Particularly in light of shrinking government investment in NASA, it is clear that future exploration and settlement of the Moon will require structural materials which can be produced cheaply, in whole or in part from locally available resources; namely, the lunar regolith. Various methods of producing structural materials from the regolith have been tested, including "lunar concrete" mixtures (Omar, 2009) and compaction of the regolith (Guerrieri et al., 1993).

But one way of producing such materials is to sinter the lunar regolith, producing dense products which can then be used to build structures such as launch pads, radiation shielding, or thermal wadis. By sintering, we mean that the material is heated to some temperatures *below* its melting point, allowing atoms to diffuse across grain boundaries and fuse them together to create a final, solid product. Regolith is a thermally inert material, and thus requires a significant amount energy for sintering to occur. Nonetheless, several methods have been successfully demonstrated to accomplish just that, including microwave radiation (Meek and Taylor, 2005), solar concentration (LPI, 1998), and sintering via self-propagating high-temperature synthesis (SHS) (Faeirson et al., 2008), also called combustion synthesis. This latter approach is the subject of this paper.

1.1 SHS: History, Characteristics, and Benefits

The concept of combustion via SHS is that a sufficiently exothermic reaction, once started, can reach temperatures high enough for the propagation of the combustion wave to become self-sustaining (Mukasyan, 2004). Thermite mixtures are a prime example of such reactions, with the typical thermite mixture consisting of a metal oxide and a metal powder as reactants. For example, the oxidation-

reduction reaction of iron(III) oxide (commonly called rust) and aluminum powder is described by the equation:

$$Fe_2O_3 + 2Al \rightarrow Al_2O_3 + 2Fe$$

This reaction often reaches temperatures of over 2500°C, more than enough to sustain propagation of the combustion wave and hot enough that it has been applied to exothermic welding of railroad tracks (Feng and Moore, 1995a).

Although in practice SHS reactions typically require a significant energy input to ignite, it is small compared to the energy released by the reaction and the propagation of the combustion wave makes the energy cost largely independent of the mixture mass. The temperatures reached are coupled with volumetric expansion, resulting in material that is extremely light, porous and heat-resistant, making it suitable for some applications. The purity of the material is also enhanced, since the combustion eliminates most volatiles present in the reactant mixture (Feng and Moore, 1995a).

An SHS reaction therefore constitutes a simple process which requires little energy relative to the heat generated by the reaction, and which can be performed cheaply without very specialized equipment.

1.2 SHS on the Moon

Much of the lunar regolith is composed of oxygen-bearing minerals (Wänke, 1974), making it a good candidate for a thermite-type reaction. But even as a diluent within a pyrotechnic mixture, temperatures can be achieved which will sinter the regolith with only modest energy requirements and create dense materials which may be suitable for structural applications. Metal powders would still be necessary for the reaction, but would constitute only a fraction of the reactant mass.

If we only desired high temperatures, it is entirely feasible to simply concentrate enough solar energy at a point and achieve sintering of the lunar regolith without the costly effort of transporting or extracting metal powders. However, SHS reactions have the added benefit of being adaptable to any given geometry, so that even very large or very complex structures can be formed merely by placing the required mixture into a mold and igniting it. The time required for the reaction to complete is short, and because these reactions rely on many different physical parameters (grain size, mixture ratio, density), it is possible to control for many of the characteristics of the final product.

One of many issues that must be addressed is that of variability: The lunar regolith is far from being uniform in composition, and samples of lunar material are unavailable for experimentation. Terrestrial simulants have been developed to satisfy the needs of researchers (Schrader et al., 2010) and are based on analysis of samples returned from the Apollo missions. Different simulants have been developed to simulate different characteristics of the lunar regolith, depending on the application, but currently the most common simulant is JSC-1A. It is based on the earlier JSC-1, and is tailored so that its particle size distribution and bulk composition are a close match to that of a typical lunar mare sample but with lower titanium concentration. Its bulk composition is shown in Table 1.2 (NASA, 2007). It is important to understand that the bulk composition is the result of *element* analysis and is intended as a way of visualizing how elements are distributed in a sample; it is not representative of the actual mineral phases present.

Table 1.2: Bulk Composition of JSC-1A

Oxide	% Mass (JSC-1A)
SiO_2	47.1
TiO_2	1.87
Al_2O_3	17.1
Fe_2O_3	3.41
FeO	7.57
MgO	6.9
MnO	0.18
CaO	10.3
Na_2O	3.3
K_2O	0.86
P_2O_5	0.76
Total	99.35

Experiments performed recently by Martirosyan and Luss at the University of Houston have demonstrated that the triple mixture of JSC-1, titanium and boron is combustible and achieves sintering with the inert JSC-1 composing 60% of the mixture. However, while titanium is at least present on the lunar surface, it is chemically bound within a mineral whose abundance is low. Worse, boron isn't present in the lunar regolith at all, so transporting it from Earth would be a necessity for this method to be feasible. Other such mixtures could certainly be tried, and many have similar problems.

Another approach was discovered by Faeirson and Logan at Virginia Polytechnic University when they demonstrated that mixtures of JSC-1AF (made from the fraction of JSC-1A below 20 μm) and aluminum will react with one another to form dense products comparable in strength to terrestrial concrete (Faeirson and Logan, 2010). Our own experiments at the University of Texas at El Paso

(UTEP) have demonstrated that mixtures of magnesium and JSC-1A also react to form dense products, and that they are easier to ignite. Both aluminum and magnesium are abundant within the oxide minerals within lunar regolith, but can also be readily scrapped from structures and vehicles already on the lunar surface.

As noted above, along with Al, magnesium could be used as a reacting metal. To our knowledge, combustion of Mg/regolith mixtures has not been studied. Note that due to the non-protective oxide layer on the surface of Mg and a relatively low boiling point of Mg (1363 K at 1 atm *vs.* 2792 K for Al), it is usually easier to ignite Mg than Al. More specifically, the ignition of Al particles may require higher temperatures (Luss and Martirosyan, 2006) or use of expensive nanoscale particles (Shafirovich and Varma, 2007). The ignition problems may be important in the combustion of lean metal mixtures, which are of interest for ISRU applications (the metal additive should be minimal).

This thesis explores the combustion synthesis of JSC-1A and magnesium, the results of thermodynamic calculations, the results of combustion experiments and the effect of gravity on combustion products.

2. Thermodynamic Calculations

Prior to combustion experiments, thermodynamic analysis was conducted using THERMO 4.2, which features a thermochemical database of over 3000 compounds and is capable of determining the equilibrium products of a reaction. To do this, it solves for the products using thermal, chemical, and phase equilibrium, which requires that the free energy of the reaction be minimized (Shiryaev, 1995). The inputs are the chemical formulas of the reactants, their molar quantities, initial conditions for all reactants (temperature and pressure), as well as formation enthalpies for any compounds not present in the database. It is assumed that combustion is adiabatic and that the mixture is homogeneous.

2.1 Techniques Using THERMO Software

Initial thermodynamic calculations were conducted using the bulk composition, shown in Table 1.2, but better accuracy was gained by using JSC-1A's mineral composition. The results of QEMSCAN data, in conjunction with the simulant characterization provided by Orbitec, were used to piece together the mineral composition of JSC-1A, shown in the third column of Table 2.1a.

THERMO is limited by the number of compounds it can process, and because of this the model composition applied in the calculations neglects many of the lesser compounds---with the exception of components which were end members of solid solutions---along with MgFeAl silicate, for which no formula was given (Botha et al., 2008), and glass, for which there is no stoichiometric representation but which was *assumed* to behave similarly to the crystalline portion of the material. The resulting composition was normalized so that the remaining minerals retained their ratios relative to one another. This model system's composition is shown below.

Table 2.1a: Comparison of JSC-1A Composition and Model System

Mineral	Formula	JSC-1A composition, wt %	Model regolith system composition, wt %
Anorthite	$CaAl_2Si_2O_8$	26.48	37.95
Albite	$NaAlSi_3O_8$	11.35	16.27
Orthoclase	$KAlSi_3O_8$	0.07	0.10
Wollastonite	$CaSiO_3$	7.77	11.14
Enstatite	$MgSiO_3$	7.38	10.58
Ferrosilite	$FeSiO_3$	4.28	6.13
Forsterite	Mg_2SiO_4	9.08	13.02
Fayalite	Fe_2SiO_4	3.36	4.81
Glass		26.67	0
MgFeAl		3.06	0
Troilite	FeS	0.17	0
Ilmenite	$FeTiO_3$	0.11	0
Magnetite	Fe_3O_4	0.01	0
Quartz	SiO_2	0.01	0
Others		0.07	0
Total		99.98	100.00

Since the database of THERMO software does not include albite and ferrosilite, the formation enthalpies of these compounds, -3,929.86 kJ/mol and -1,193.45 kJ/mol, respectively, were taken from Saxena, 1997.

2.2 Results

Figure 2.2a shows the obtained adiabatic flame temperatures for the mixtures of the model regolith system with aluminum and magnesium. For Al, the maximum adiabatic flame temperature,

1566 K, is observed at 23 wt% metal. For Mg, the maximum is equal to the melting point of silicon, 1690 K, which is present in the combustion products. This temperature plateau is observed in the range from 26 wt% to 39 wt% Mg. It is seen that Mg-based mixtures exhibit a higher temperature than Al-based ones at all metal concentrations. Specifically, for lean metal mixtures, the adiabatic temperature for Mg is higher by more than 100 K than that for Al in the range from 8 wt% to 17 wt% metal. The maximum temperature for Mg is higher by 124 K than that for Al. These observations, as well as the aforementioned data on easier ignition of Mg particles (Shafirovich and Varma, 2007), imply that Mg/regolith mixtures may burn better than Al-based ones.

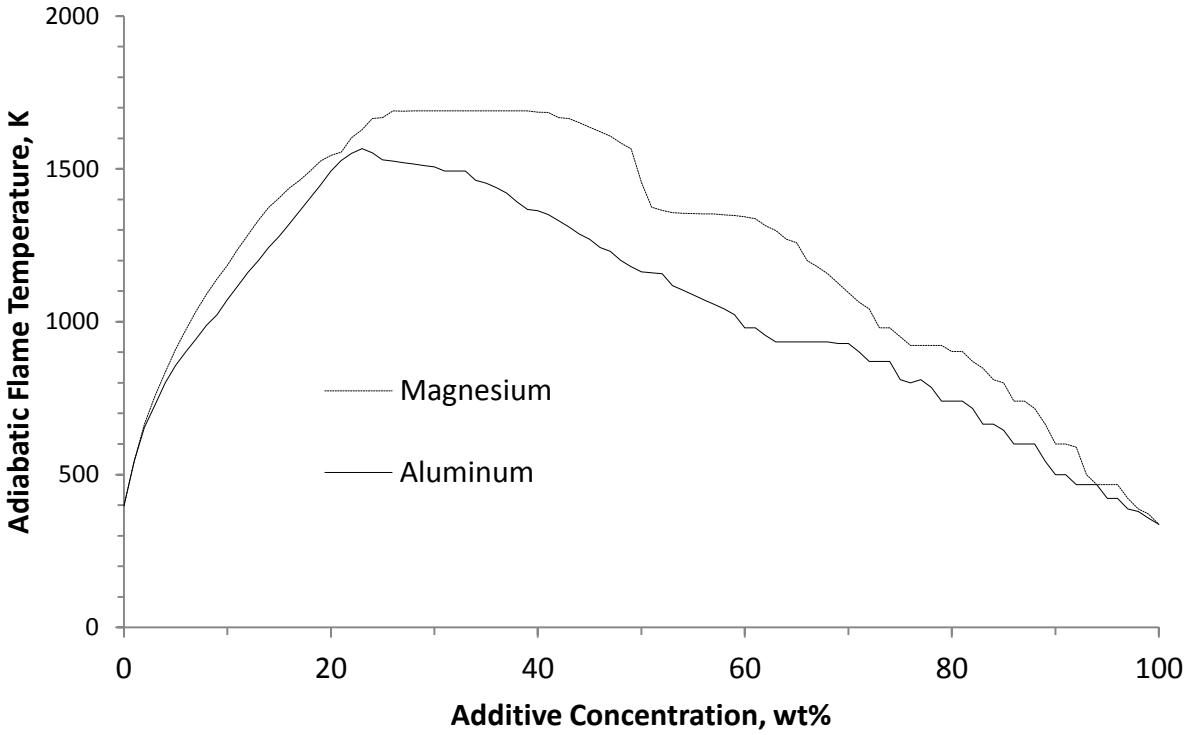

Figure 2.2a: Calculated temperatures of combustion of magnesium and aluminum with JSC-1A as a function of metal concentration.

The product compositions of the mixtures with 23 wt% Al and 26 wt% Mg are shown in Tables 2.2a and 2.2b, respectively. The results for the Al-based mixture are in a qualitative agreement with the experiments (Faeirson, 2009), where silicon, grossite (CaAl4O7), gehlenite (Ca2Al2SiO7), spinel

(MgAl2O4), corundum (Al2O3), and fersilicite (FeSi) were identified by X-ray diffraction analysis in the combustion products of JSC-1AF lunar regolith simulant mixed with 24.45 wt% Al.

Table 2.2a: Combustion products of Al/JSC-1A mixture; 23 wt% Al, pressure: 1 atm

Formula	Phase	Composition, wt%
$MgAl_2O_4$	Solid	35.42
$CaAl_4O_7$	Solid	21.05
Si	Solid	16.19
$Ca_2Al_2SiO_7$	Solid	11.59
FeSi	Liquid	11.47
Al_2O_3	Solid	1.77
$NaAlO_2$	Gas	1.66
K	Gas	0.78
Na	Gas	0.03

Table 2.2b: Combustion products of Mg/JSC-1A mixture; 26 wt% Mg, pressure: 1 atm

Formula	Phase	Composition, wt%
$MgAl_2O_4$	Solid	35.42
$CaAl_4O_7$	Solid	21.05
Si	Solid	16.19
$Ca_2Al_2SiO_7$	Solid	11.59
FeSi	Liquid	11.47
Al_2O_3	Solid	1.77
$NaAlO_2$	Gas	1.66
K	Gas	0.78
Na	Gas	0.03

An apparent advantage of using Al and Mg is the formation of silicon as a byproduct. Silicon could be separated from the combustion products using its relatively low melting point (1690 K) and used for the fabrication of solar cells.

Verifying whether magnesium mixtures achieve higher temperatures than aluminum mixtures requires some knowledge about how those components of JSC-1A neglected in the calculations will behave. The assumption that glass, in particular, will have similar composition to the crystalline part of the regolith simulant may cause some error. It may be more accurate to represent the glass as a mixture of simple oxides, as shown in the second column of Table 2.2c (Hill et al., 2007).

Table 2.2c: Composition of Glass in JSC-1A

Oxide	Glass Composition, wt%	Model Glass System Composition, wt%
SiO_2	46.8	49.81
TiO_2	2.44	0
Al_2O_3	13.9	14.79
FeO	12.1	12.88
MgO	5.6	5.96
MnO	0.21	0
CaO	10.5	11.17
Na_2O	3.89	4.14
K_2O	1.17	1.25
P_2O_5	1.04	0
TOTAL	97.7	100.00

Unfortunately, THERMO cannot calculate for the system that includes both the mineral phases of the regolith and the simple oxides contained in the glass; there are simply too many components in the initial mixture. For this reason, we conducted additional calculations where the regolith was replaced by glass, i.e., by the mixture of simple oxides shown in the third column in Table 2.2c. Since the glass is 26.67 wt% of JSC-1A, the actual results would likely be amid those obtained on the assumption that the glass is the same as the mineral part and those obtained on the assumption the regolith is 100% glass.

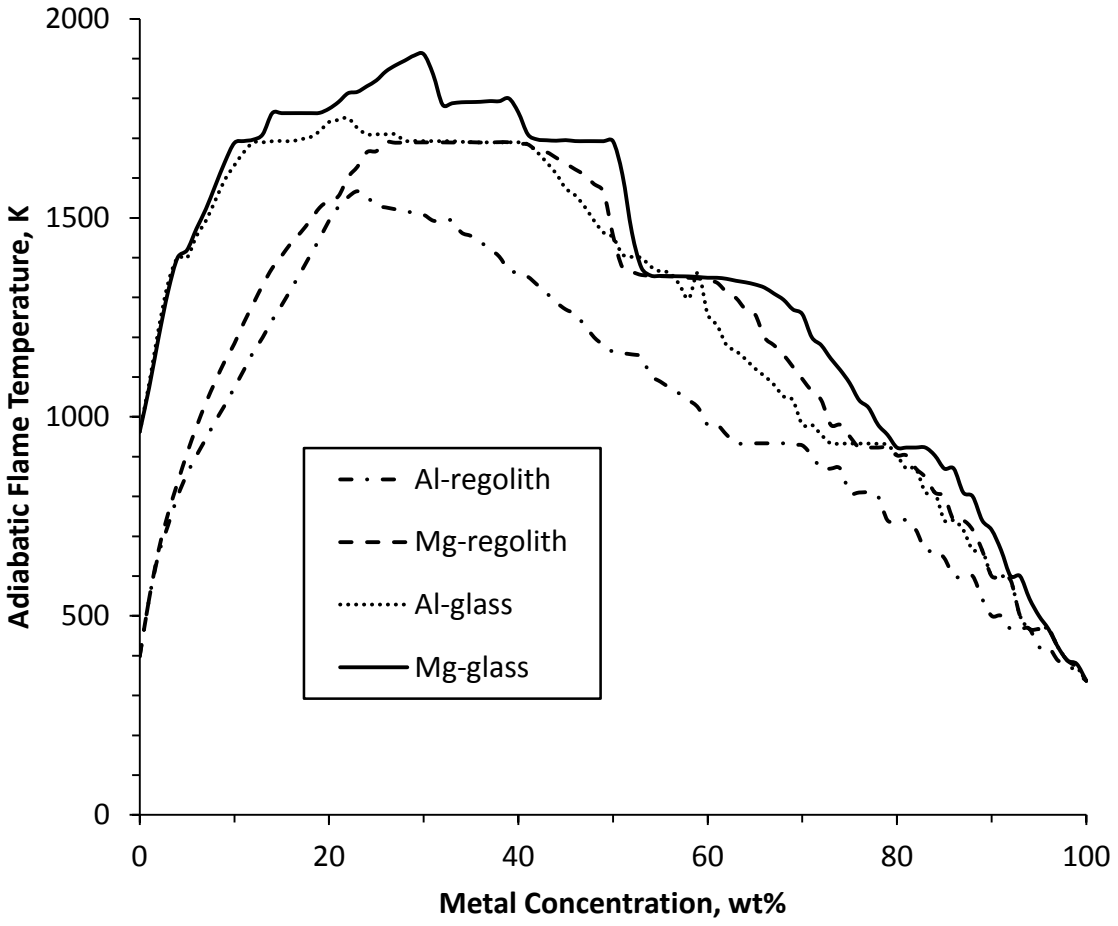

Figure 2.2b: Calculated temperatures of combustion of magnesium and aluminum with the glass component of JSC-1A as a function of metal concentration.

Figure 2.2b shows the obtained adiabatic flame temperatures for the mixtures of the model glass system with aluminum and magnesium in comparison with the results obtained for the model regolith system. For both Al and Mg, the maximum adiabatic flame temperature is higher by 200 K in the case where the regolith is 100% glass. Also, in this case there are rather wide concentration ranges where the adiabatic temperatures are close to maximum values. The conclusion on higher temperatures for Mg as compared with Al thus remains valid. As noted above, the actual curves would possibly be located between those for glass and regolith (closer to the latter curves as the glass content is only 26.67 wt%).

Tables 2.2d and 2.2e show the combustion products of glass/Al and glass/Mg mixtures at the same metal concentrations as in Tables 2.2a and 2.2b. It is seen that the replacement of mineral phases by simple oxides in the initial mixture leads to changes in the mineral compositions of the products, especially in the case of Al.

Table 2.2d: Combustion products of Al/glass mixture at 1 atm

Formula	Phase	Composition, wt%
Al_2O_3	Solid	35.42
$Ca_2Al_2SiO_7$	Solid	21.05
$MgAl_2O_4$	Solid	16.19
FeSi	Solid	11.59
Si	Liquid	11.47
Na_2SiO_3	Solid	1.77
Na	Gas	1.66
K	Gas	0.78
Na_2	Gas	0.03
SiO	Gas	0.02
KNa	Gas	0.02

Table 2.2e: Combustion products of Mg/glass mixture at 1 atm

Formula	Phase	Composition, wt%
MgO	Solid	35.42
$MgAl_2O_4$	Solid	21.05
Ca_2SiO_4	Solid	16.19
Si	Solid	11.59
FeSi	Liquid	11.47
Na	Solid	1.77
K	Gas	1.66
Mg	Gas	0.78
SiO	Gas	0.03
Na_2	Gas	0.02
KNa	Gas	0.02

These results are meaningful only if the glass behaves similarly to simple oxides, however. Analysis of the actual combustion products will determine whether the initial assumption was true, that the glass behaves similarly to the crystalline portion of the simulant, or whether it is more accurate to assume it to be composed of simple oxides. These results are discussed in this paper, starting on page 27.

3. Experimental Studies

3.1 Experimental Setup

The combustion experiments with Mg/JSC-1A mixtures were conducted in a windowed steel chamber (diameter 30 cm, height 40 cm), connected to a compressed argon cylinder and a vacuum pump (Rocker 300), as shown in Figure 3.1a and Figure 3.1b. During the experiment, a pellet of the tested mixture was installed on a brass pedestal inside the chamber and ignited at the top by a Nichrome wire connected to a DC power supply (Mastech HY3020E), as shown in Figure 3.1c. Video recording (Samsung MiniDV DigitalCam) was used for observation of the combustion process. The experiments were conducted in argon environment at atmospheric pressure (approximately 90 kPa) and at reduced pressure (approximately 10 kPa).

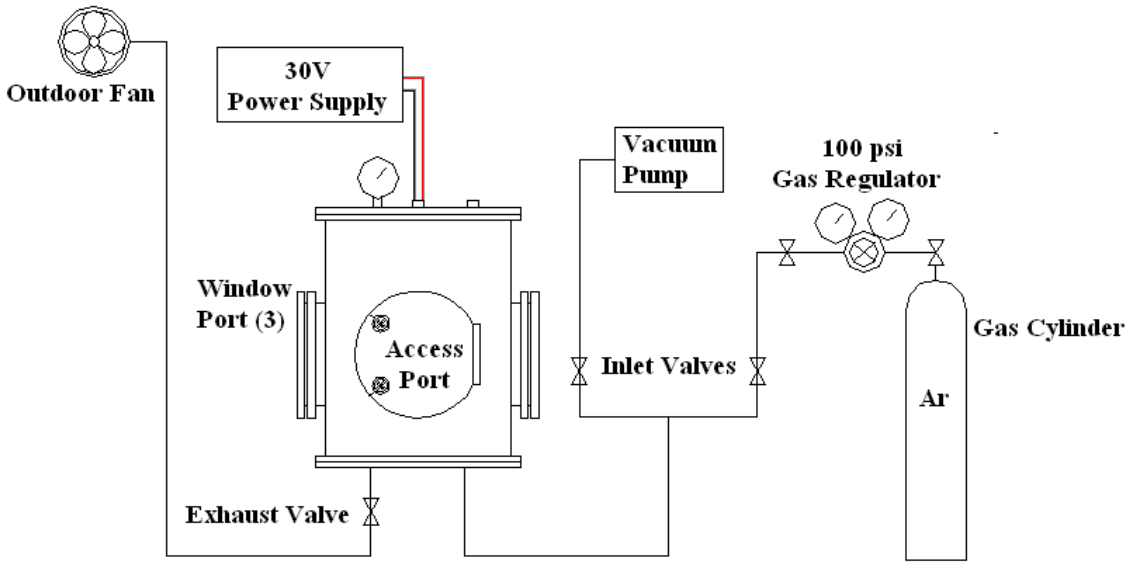

Figure 3.1a: Design of the experimental setup.

Figure 3.1b: Photograph taken of the experimental setup.

The samples were to be cylindrical pellets with a diameter of 13 mm and a height of 1-2 inches. A brass mount was machined to hold the pellet samples, and two brass terminals were used to hold igniters. These terminals were linked to the power supply via feed-thrus in the chamber.

Figure 3.1c: Photograph of the inside of the combustion chamber.

The setup was modified for experiments in reduced gravity. Instead of a vacuum pump, an onboard vent was used to take advantage of the pressure difference between the inside and outside of the cabin while argon flushed the chamber. A rotating sample cartridge was installed inside the chamber, and additional feed-thrus were added to accommodate 15 samples per flight.

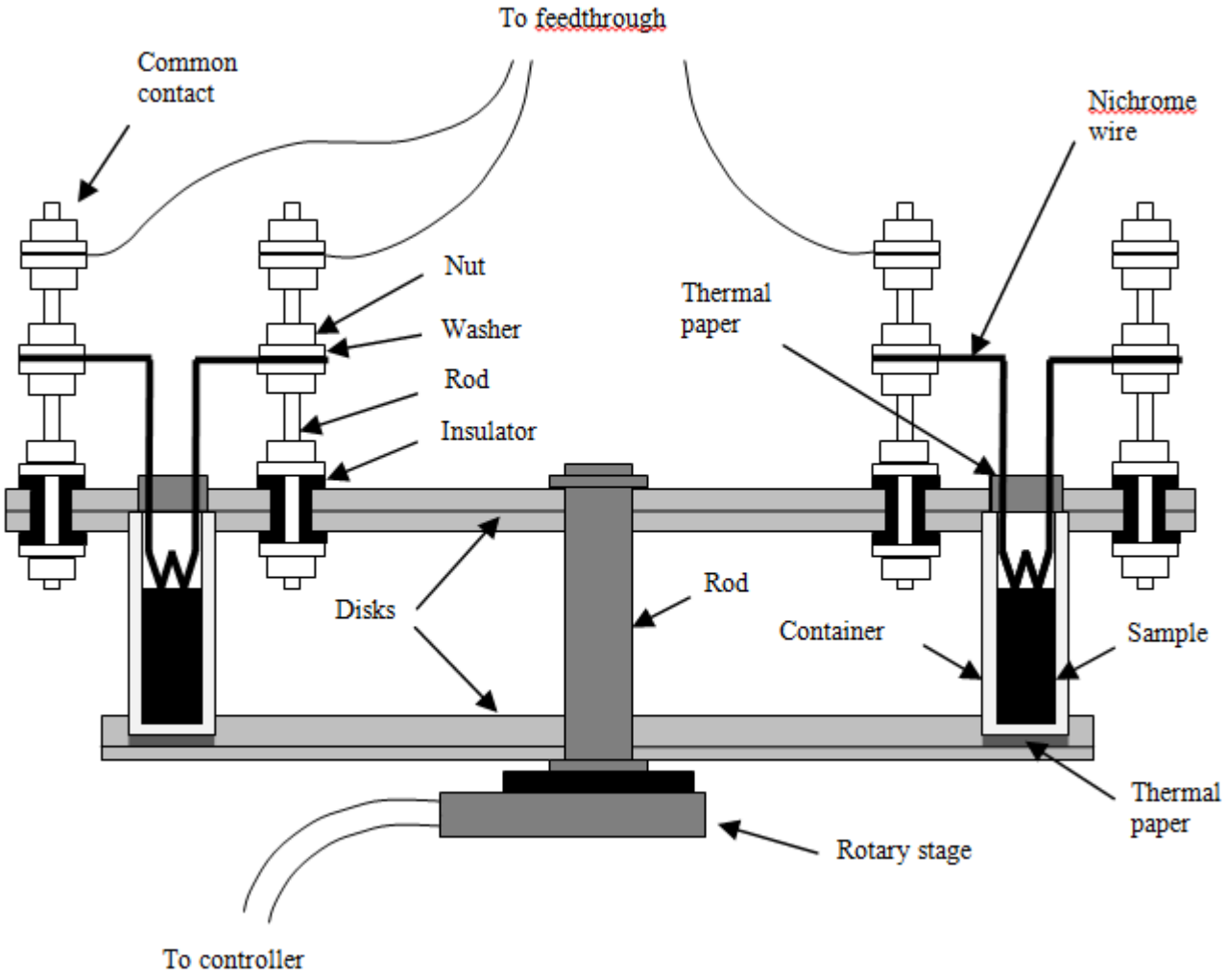

Figure 3.1d: Design of rotating sample cartridge used in reduced gravity experiments.

Samples for reduced flight experiments used JSC-1A (milled by PBM) in a 26% Mg mixture which was lightly compressed.

3.2 Preparation of Samples

JSC-1A lunar regolith simulant was obtained from Orbitec. Initially, this powder was used as received but the attempts to ignite its mixtures with Mg failed. This is apparently associated with a relatively large particle size of the used simulant. To increase the specific surface area of this powder and thus increase the reaction rate between the regolith simulant and the metal, the former was ground in a roller ball mill (Labmill-8000). The powder sample, 20 g, was placed in an alumina-fortified porcelain jar (U.S. Stoneware) with 5 cylindrical (diameter 1.3 cm, height 1.3 cm) BurundumTM (alumina) grinding media. The rotation speed was approximately 200 rpm and the milling time was varied from 1 h to 20 h.

Magnesium (-325 mesh, i.e. less than 44 μm, 99.8% pure) powder was obtained from AlfaAesar and used as received. The original and milled JSC-1A powders were mixed with the magnesium powder using the aforementioned roller ball mill. The powders were placed in a polyethylene container with 5 BurundumTM cylinders. The mixing time was 5 min. The Mg/JSC-1A mixture ratio corresponded to the value of 26 wt%, which, according to the thermodynamic calculations (Section II), provides the maximum adiabatic flame temperature. The mixture samples were compacted into pellets (diameter 1.3 cm, height 2.9-3.7 cm) using a hydraulic press (the pressing force 8.9 kN).

3.3 Results of Particle Size Analysis

As stated before, early attempts to ignite JSC-1A with magnesium were unsuccessful, either because the flame did not propagate to the end of the sample of because the sample did not ignite at all. It was believed that by decreasing the average grain size, mixtures could be more readily ignited. As a preliminary test, the grain size of JSC-1A lunar simulant was measured by sieving 100 g of material.

Milled samples were sieved in 20-g batches due to the impracticality of milling large amounts. The results are shown in Figure 3.2a.

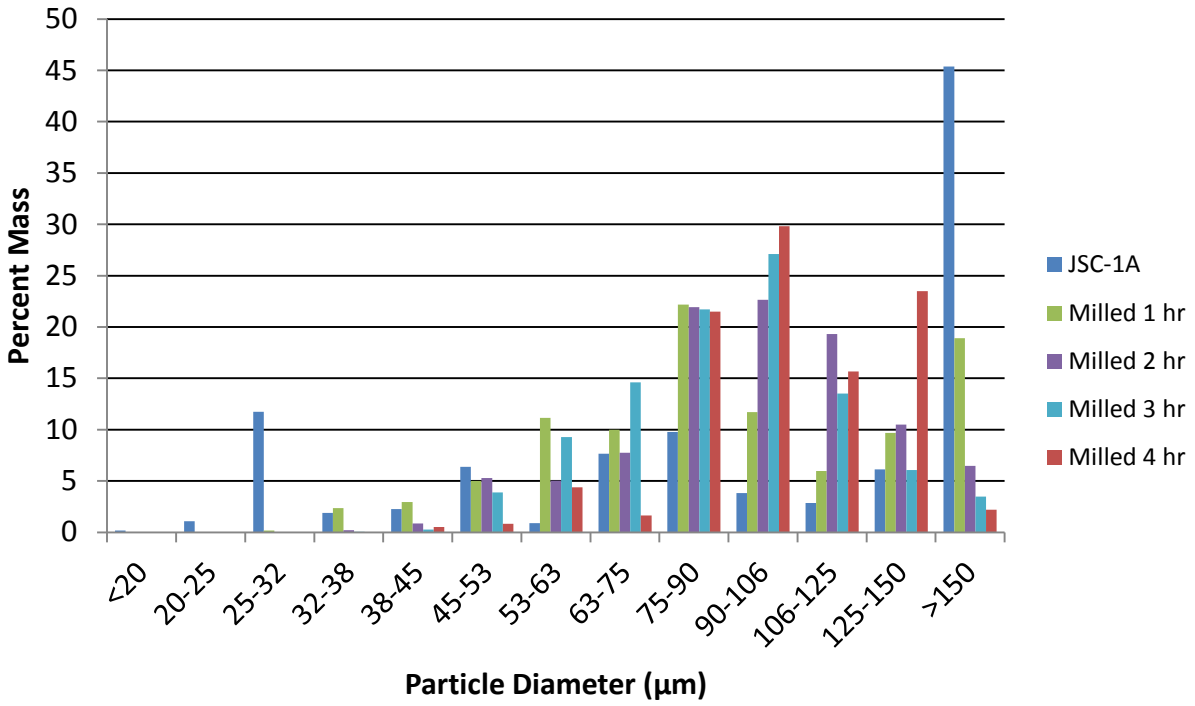

Figure 3.2a: Results of sieving for JSC-1A and milled samples.

It is expected, of course, that the average particle size should decrease with milling. This decrease is offset in the sieve measurements by agglomeration of smaller particles as they are milled (caused partly by charges imparted to the particles during milling), so the sieving measurements are not nearly as accurate as desired. Agglomeration of particles became clearly visible when samples were milled at least 3 hours and became more pronounced the longer the samples were milled.

For better results, laser diffraction was applied using water and L-1 sodium hexametaphosphate (a dispersing agent) as the carrying fluid. For samples milled from 1 to 20 hours, results can be found in the Appendix.

It must be understood first that particle size measurements take different forms. We customarily assume the particles to behave like spheres, even if their shape is far from spherical, and substitute for the diameter either the average maximum or minimum length across a set of particles, or else a diameter derived from the surface area, volume, or some combination of parameters. In the case of sieving, particle shape can significantly skew the results.

Our laser diffraction measurements show two forms of the mean diameter: D[4,3] and D[3,2], or the volume-weighted mean and the surface-weighted mean, respectively. For a given sample of particles $\{p_1, p_2, p_3, \dots, p_n\}$ with diameters $\{d_1, d_2, d_3, \dots, d_n\}$, D[4,3] and D[3,2] are given by:

$$D[4,3] = \frac{\sum_{i=1}^{n} d_i^4}{\sum_{i=1}^{n} d_i^3}$$

$$D[3,2] = \frac{\sum_{i=1}^{n} d_i^3}{\sum_{i=1}^{n} d_i^2}$$

The volume-surface mean is often used in applications where the surface area of the particles is of interest, such as in combustion, but the volume-moment mean is more often reported in literature. Both are included here.

Following are the particle size distributions taken for JSC-1A using water and L-1 sodium hexametaphosphate as the carrier fluid, as well as the distribution for a sample milled for five hours. Shown below is a plot of the original size distribution and that of a sample milled for five hours. Note alterations in the shape and range of the size distribution with milling time.

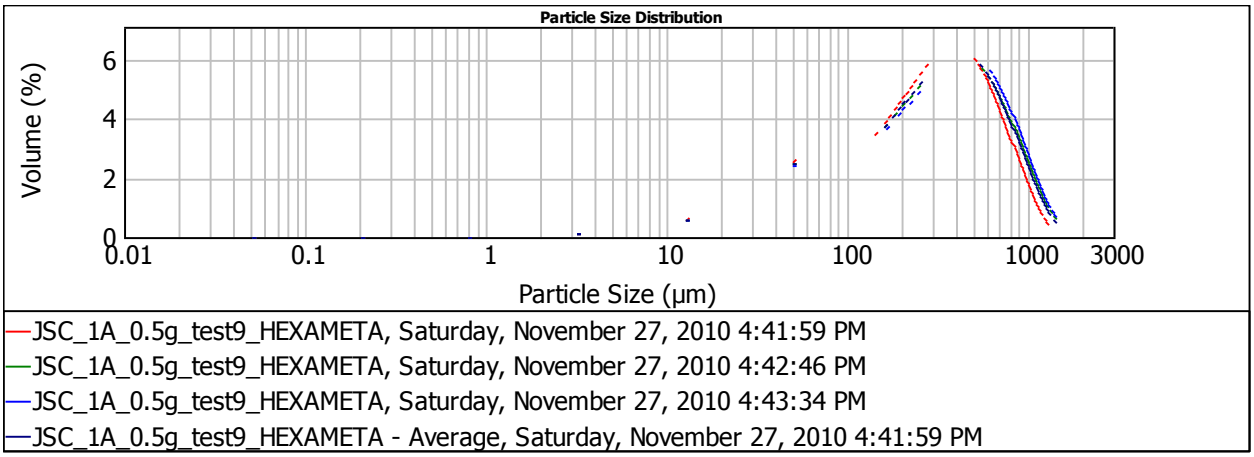

Figure 3.2b: Particle size distribution of JSC-1A.

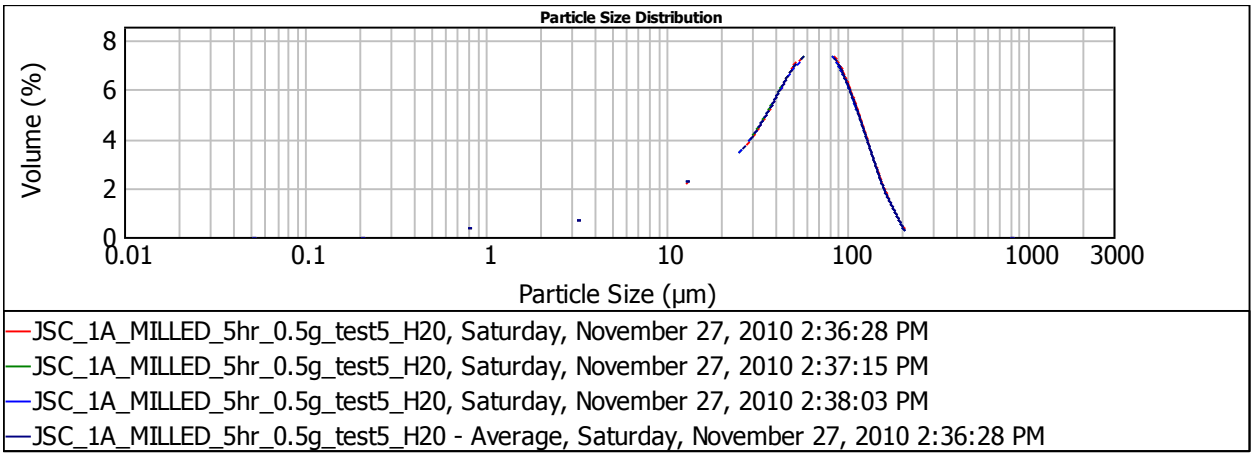

Figure 3.2c: Comparison of size distributions for original JSC-1A and a sample milled 5 hours.

Figure 3.2d shows the influence of the milling time on the volume weighted mean particle size, surface weighted mean particle size, and count-median diameter.

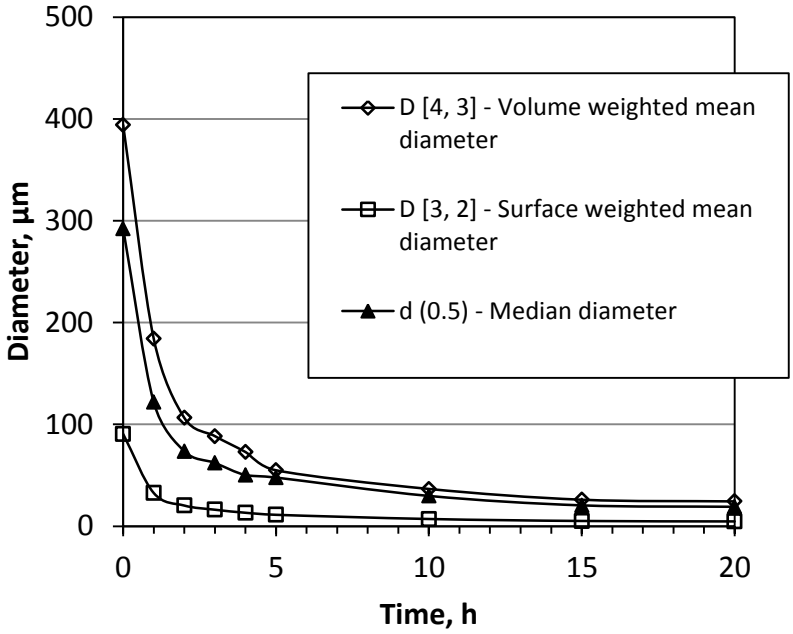

Figure 3.2d: Effect of milling on particle diameter as a function of milling time.

D[3,2] is used by laser diffraction software to calculate the specific surface area (surface area of particles per unit volume), using the equation:

$$SSA = \frac{6}{\rho D[3,2]}$$

This results in the following plot:

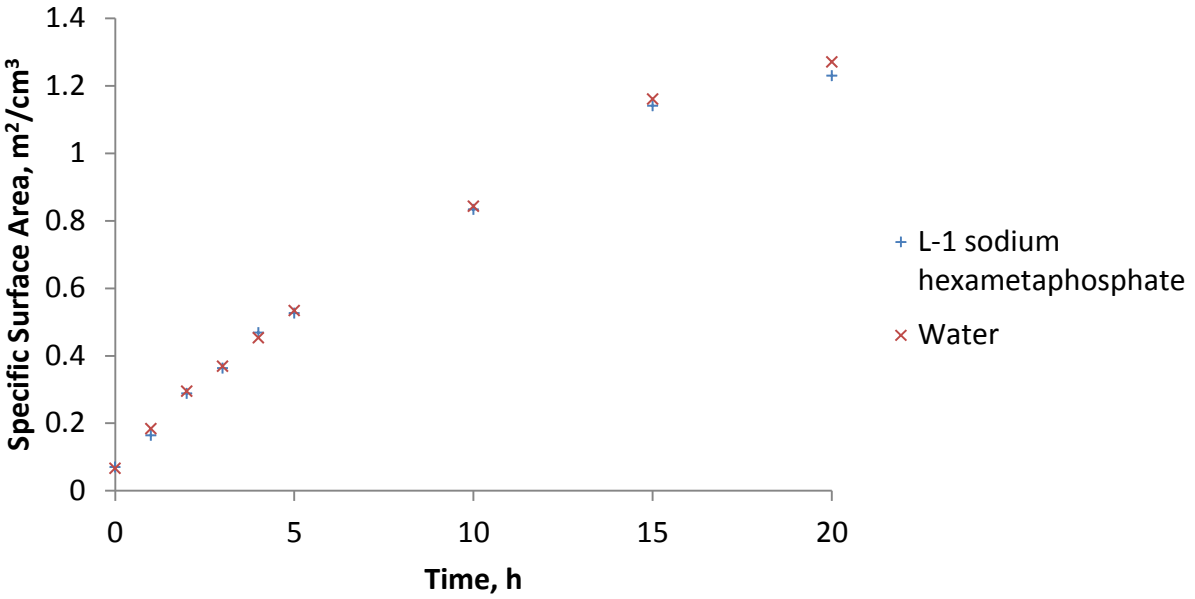

Figure 3.2e: Effect of milling on surface area.

Milling for 5 h and 20 h increases the specific surface area of JSC-1A by a factor of 8 and 19, respectively.

Figure 3.2f shows the relative density of the mixture samples as a function of the milling time of JSC-1A. The relative density is defined as a ratio of the measured sample density to the theoretical density of a non-porous sample. Since the density of Mg is 1.74 g/cm^3 and, according to the literature (Agui et al., 2010), the density of JSC-1A material is 2.9 g/cm^3, the theoretical density of the mixture of 26 wt% Mg and 74 wt% JSC-1A is equal to 2.6 g/cm^3.

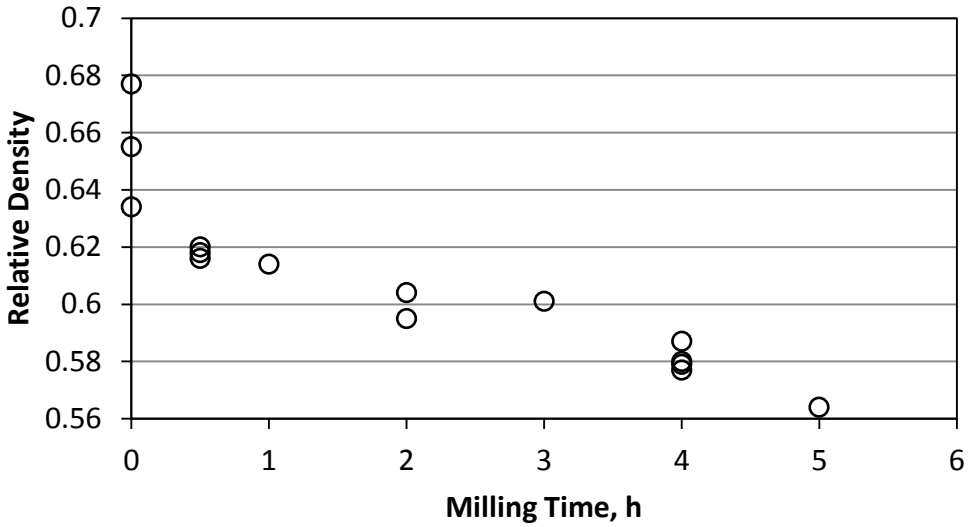

Figure 3.2f: Effect of milling on relative density of pressed samples.

The results presented in Figure 3.2f indicate that increasing the milling time of JSC-1A decreases the relative density of the compacted Mg/JSC-1A mixtures. This effect is apparently associated with narrowing the particle size range due to grinding, which is illustrated by comparison of the particle size distribution for the powder milled for 5 h (Figure 3.2c) with that for the original JSC-1A (Fig. 3.2b). Quantitative comparison of the particle size distribution widths can be made using the equivalent diameters D10 and D90 (diameters for which 10 wt% and 90 wt% of the particles have a smaller diameter). For the unmilled powder D10 = 36.1 μm and D90 = 908.9 μm, while for the powder milled for 5 h, D10 = 6.5 μm and D90 = 113.9 μm. Comparison of (D90 – D10) values and also of D90/D10 ratios clearly shows that milling narrows the particle size distribution. When the particle size range is narrower, the porosity of the mixture is higher and the relative density is lower.

A Fritsch planetary ball mill (abbreviated PBM) was used to mill JSC-1A simulant to a much smaller particle size. The results of laser diffraction analysis carried out by Dr. Bonnie Cooper at Johnson Space Center shows an average volumetric diameter of approximately 5.6 μm for this powder

and an average surface-weighted mean of about 2 μm. The complete results can be found in the Appendix.

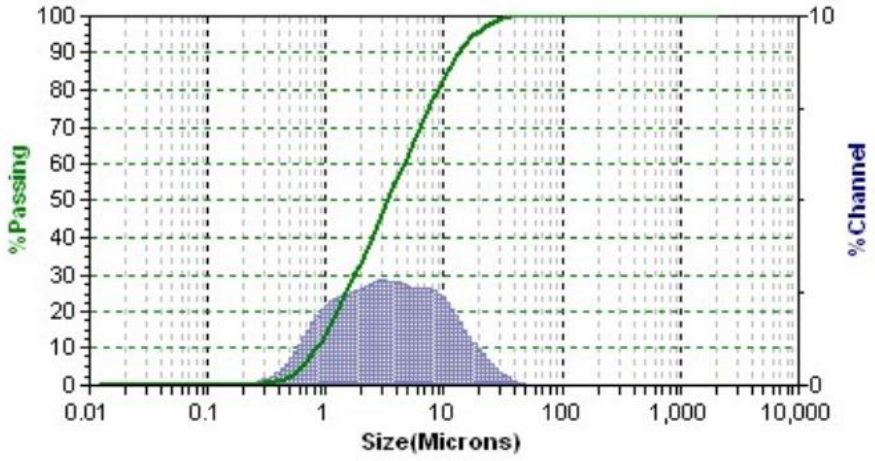

Figure 3.2g: Particle size distribution of JSC-1A milled by planetary ball mill.

Samples milled by PBM were extremely fine, and were used in reduced gravity flight experiments conducted in June 2011. Due to the small particle size, it was not feasible to press large pellets, and so powder mixtures were lightly compacted by hand and used within quartz tubes with inner diameters of 12 mm and 18 mm, all with a base and wall thickness of 1 mm.

What is important to take away from the available data is that 1) particle size decreases with milling time, 2) both the shape and range of the particle size distribution is altered by milling, 3) the specific surface area increases with milling time, and 4) milling increases the tendency of the powder to clump. These changes, in turn, affect the effectiveness of mixing, the actual force applied to samples (due to increased friction within the punch and die), the density of compressed mixtures, and their combustion behavior.

3.4 Procedure for Combustion Experiments

Experiments were conducted in an argon at local atmospheric pressure (for an elevation of 1206 m, approximately 90 kPa) and in vacuum (10 kPa). The procedure for pellet samples was as follows:

1. *Sample set-up*: The sample is placed on a brass mount and an ignition coil is connected to the igniter terminals. The chamber and all valves are then closed.

2. *Flush cycle*: The outlet valve is opened and the vacuum pump is turned on. Once the pressure has reduced to -23 inHg gauge, the vacuum pump is turned off and the outlet valve is closed. The inlet valve is opened and the gas regulator is used to allow argon to flow into the chamber until the gauge pressure reaches zero. The valves are closed. This step is done 5 times.

3. *Camera set-up*: The digital camera is placed in front of the chamber window and the focus is adjusted manually.

4. *Voltage increase*: With the current dials set to maximum current, voltage is increased by half a volt every five seconds.

5. *Combustion*: When combustion is observed, the power to the igniter is reduced to zero. If the sample does not ignite, voltage continues to be increased until the igniter coil breaks.

6. *Cooling*: The sample is allowed to cool for at least thirty minutes.

7. *Air flush*: The chamber is opened and the vacuum pump is turned on for twenty seconds to allow air to flush the chamber.

8. *Sample removal*: The vacuum pump is turned off and the sample is removed from the chamber before being stored and labeled.

The chamber remained sealed during reduced gravity flight experiments, meaning that samples were pre-loaded onto the rotary stage prior to the flight. Since there were 15 samples and 30 parabolas flown per flight, all that was necessary was to flush the chamber with argon and rotate samples during odd-numbered parabolas and ignite samples on even-numbered parabolas.

3.4 Results of Combustion Experiments

The JSC-1A powders milled for 0.5 h, 1 h, 2 h, 3 h, 4 h, and 5 h were used for the combustion experiments in 1-g, while JSC-1A milled by PBM was used for experiments in both 1 g and 0 g. In two of the three experiments conducted for the milling time of 0.5 h, ignition was not achieved, while in the third test the combustion front propagated over part of the sample height and then extinguished. At 1 h of milling, ignition and partial propagation were also observed in one of the two conducted experiments. At 2 h of milling, in two of the three experiments the propagation over the entire sample was observed. At 3 h, 4 h, and 5 h, the front propagated to the bottom in all tests. Based on these results and on the particle size characteristics for the different milling times (Figure 3.2d), it may be concluded that for stable combustion of Mg/JSC-1A mixtures, the volume weighted mean diameter of JSC-1A should be less than 100 μm (for the specific Mg powder used in the experiments).

Figure 3.4a shows typical images of combustion front propagation over the Mg/JSC-1A mixture pellet, followed by cooling of the combustion products. The time 0 in this sequence of images corresponds to the beginning of the front propagation. The top row of images demonstrates a relatively uniform propagation of the combustion front. The low row of images illustrates cooling of the sample.

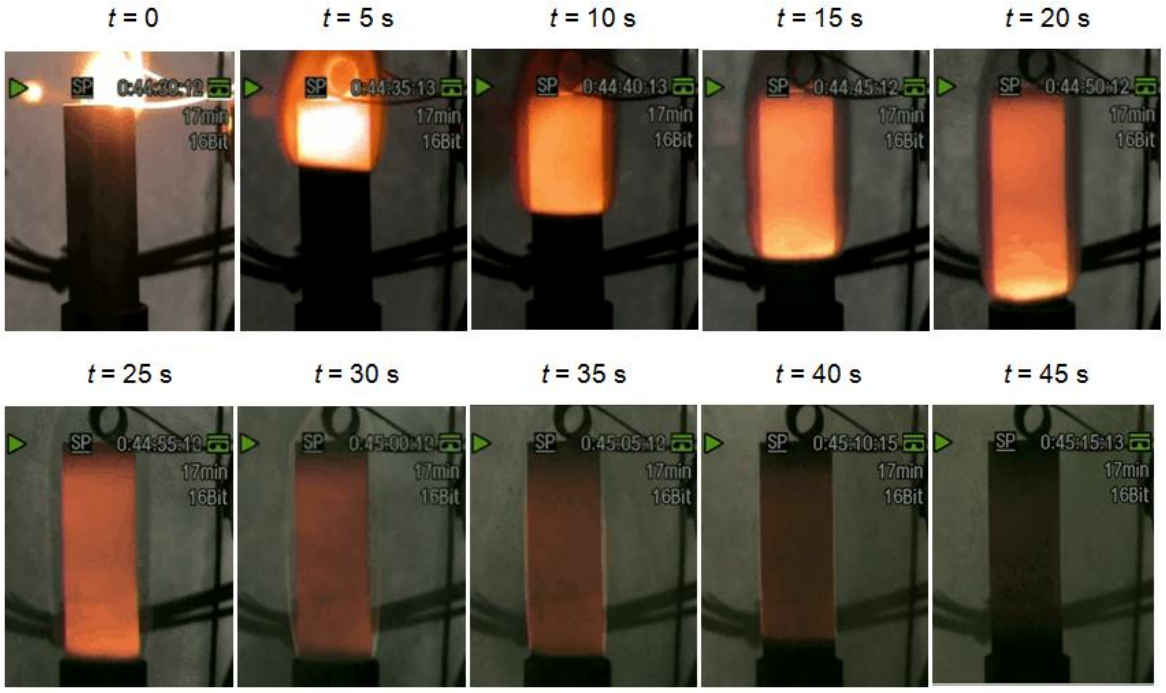

Figure 3.4a: Propagation of the combustion wave in a pressed sample.

Figure 3.4b shows the effect of the milling time on the velocity of the combustion front. To avoid unsteady effects at the top and bottom of the sample, the velocity was determined as an average velocity in the middle part of the sample height. Each point in Fig. 3.4b corresponds to a single experiment. A linear trend is observed for both pressures (10 kPa and 90 kPa). It is seen that pressure does not have an appreciable influence the combustion front velocity. This is explained by the fact that the combustion product composition of the Mg/JSC-1A mixture includes relatively small amounts of gases (see Table 2.2b).

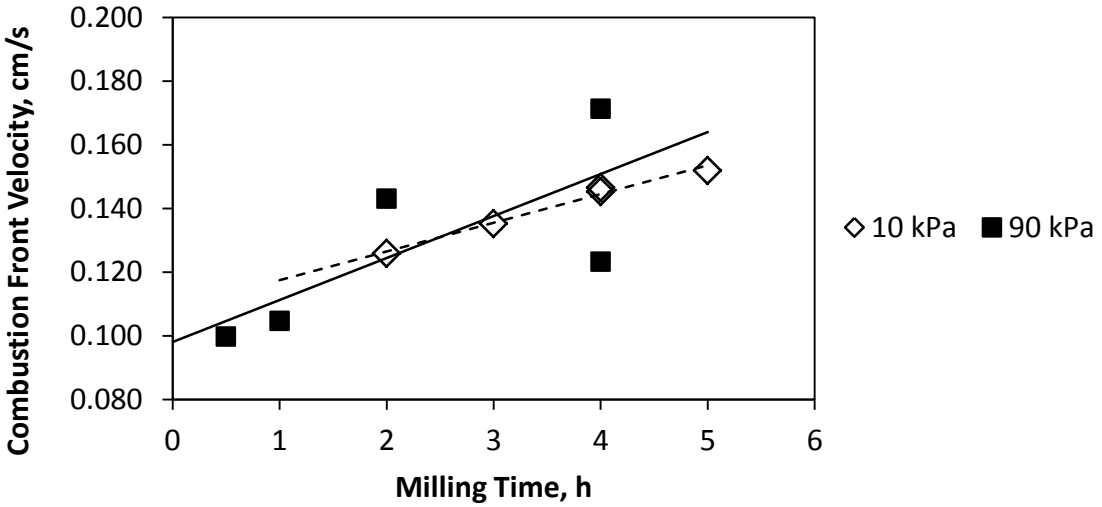

Figure 3.4b: Effect of milling on the combustion front velocity as a function of millng time.

The change in the relative density (Figure 3.2f) may influence the combustion front velocity via the change in the thermal diffusivity of the mixture (Maksimov et al., 1965) but it is difficult to evaluate this effect for the investigated system. Note that the difference between the relative densities for the powders milled for 0.5 h and 5h is less than 10%, which is too small to explain the observed 50% increase in the combustion front velocity. Apparently, the increase in the front velocity with increasing the milling time of JSC-1A is caused by the decreased particle size and correspondingly by the increased surface area of the powder.

XRD tests were performed to determine the product composition of a lightly compacted mixture composed of 26% Mg and JSC-1A (milled by PBM) burned at 1 g, and the product composition of the same mixture burned in reduced gravity.

Results for PBM-JSC-1A and 26% Mg burned at 1-g are shown in the following figures.

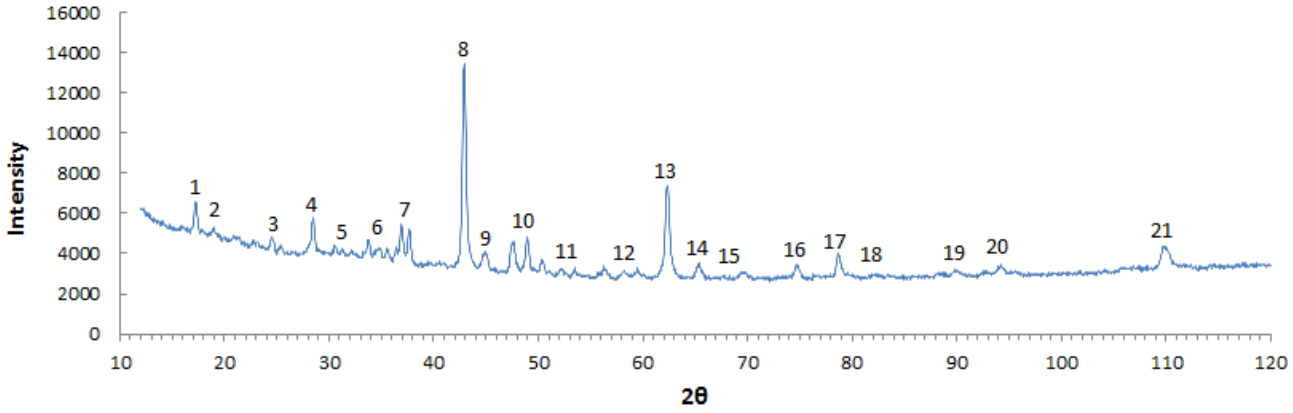

Figure 3.4c: XRD results for a sample burned at 1 g.

Table 3.1a: 1-g Products

Formula	Name	Peak Locations
$FeSi_2$	Iron silicide	1, 7, 10, 11, 15
$MgAl_2O_4$	Spinel	2, 5, 7, 9, 12, 14, 18, 20
$CaMgSiO_4$	Monticellite	3, 4, 5, 6, 7, 10, 11, 12, 15, 19
Mg_2SiO_4*	Forsterite	1, 5, 6, 11, 15
Si	Silicon	4, 10, 15
MgO	Magnesia	7, 8, 13, 16, 17, 20, 21

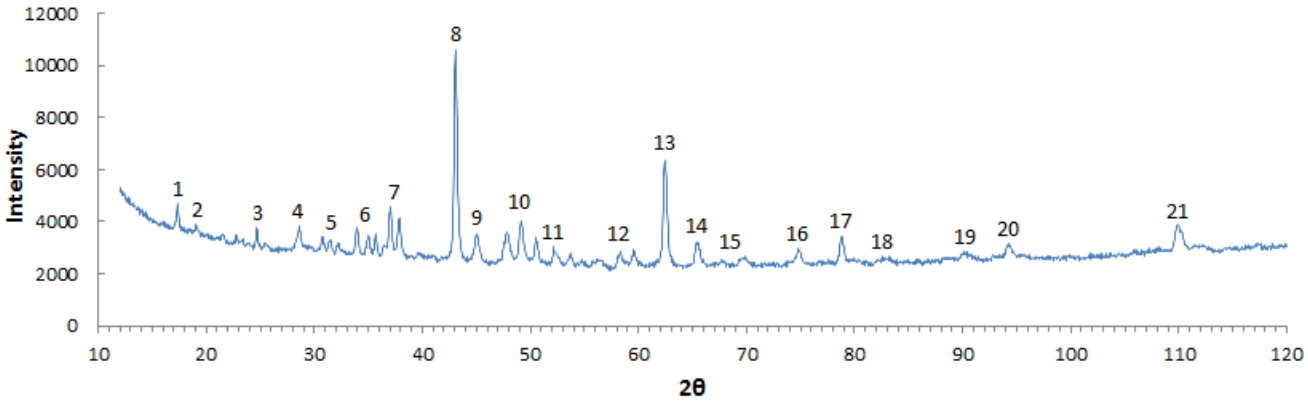

Figure 3.4d: XRD results for a sample burned in 0 g.

Table 3.1b: 0-g Products

Formula	Name	Peak Locations
$FeSi_2$	Iron silicide	1, 7, 10, 11, 15
$MgAl_2O_4$	Spinel	2, 5, 7, 9, 12, 14, 18, 20
$CaMgSiO_4$	Monticellite	3, 4, 5, 6, 7, 10, 11, 12, 15, 19
Mg_2SiO_4	Forsterite	1, 5, 6, 11, 15
Si	Silicon	4, 10, 15
MgO	Magnesia	7, 8, 13, 16, 17, 20, 21

The results were analyzed with EVA laser diffraction software, which carried out a semi-quantitative analysis of the relative intensity ratios using data from the PDF-4 database. The relative intensity (I/I_c, where I_c is the intensity of corundum) of forsterite was not found in the database, and so the value 1 was substituted in its place (likely a significant source of error). Even so, analysis of the relative intensity ratios found that the results compare well with the thermodynamic calculations.

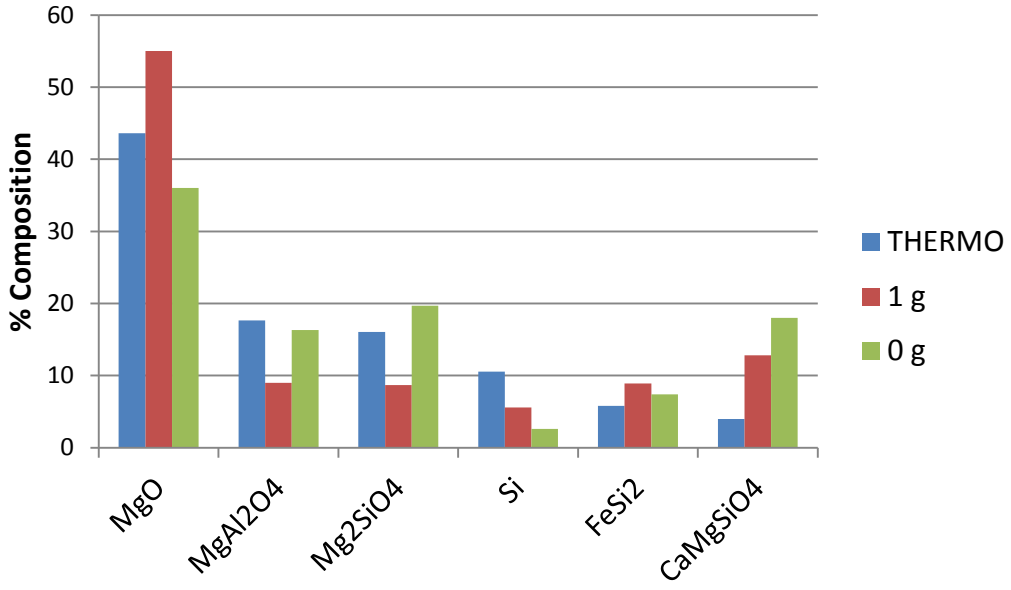

Figure 3.4e: Comparison of calculated results to actual combustion products.

The bar graph presented here is intended merely as an aid to help in visualizing the XRD results, and so is a little oversimplified. Note first that THERMO specifies calcium magnesium silicate ($Ca_3MgSi_2O_8$), not forsterite (Mg_2SiO_4), and iron silicon (FeSi) instead of iron silicide ($FeSi_2$). But geologically, there is not a terribly large difference here (two silicates of the form $Ca_xMg_y(SiO_4)_z$ and two ferrous silicon compounds), and so overall the results are in good agreement with the calculations. More important is the indication that our assumption that the glass portion of JSC-1A might behave similarly to the crystalline portion of the simulant composition is actually quite reasonable, and that the *concentrations* of different mineral phases in the products are affected by gravity.

Experiments described up to this point were performed using mixtures of 74% JSC-1A and 26% Mg, which were predicted by calculations to attain the highest temperatures. Further minimizing the cost of this technology is still a key concern, though, particularly in applications which don't require high density or strength. Experiments to determine the minimum magnesium content necessary for steady combustion were conducted.

Our prior experiments found reliable *ignition* for pressed samples of JSC-1A and Mg in which the JSC-1A had been milled for 2 hours, and steady propagation of the combustion wave in most samples even if the combustion wave stopped short of burning the entire pellet. However, pulsation during combustion in one sample suggested that the mixture was, indeed, at the lower limit of the steady combustion region. It was found that further reducing the percent composition of Mg from 26% to 23% resulted in samples which featured spin combustion. This suggests that the lowest magnesium content necessary for stable combustion is likely quite close to that required for the maximum temperature.

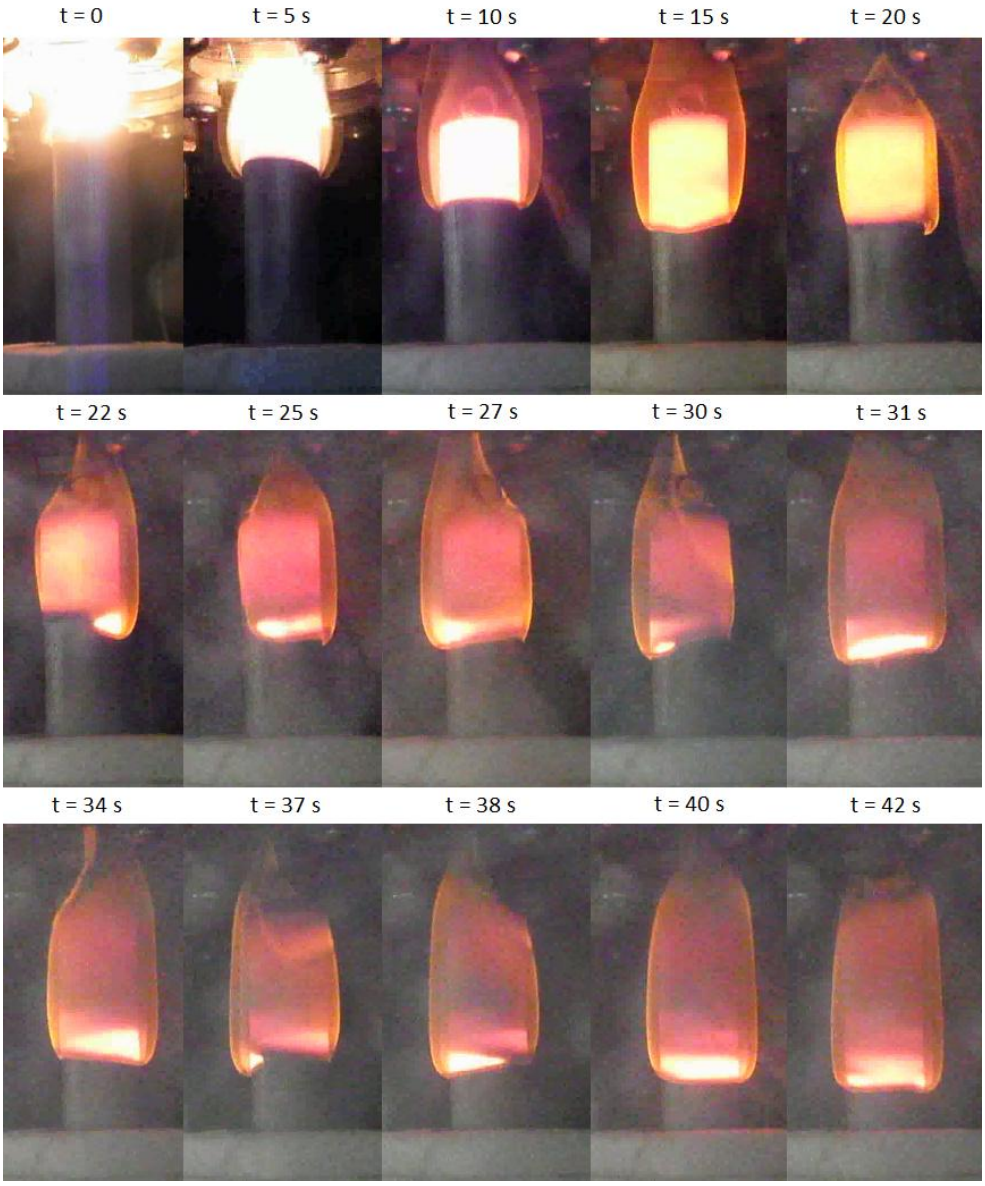

Figure 3.4f: Spin propagation in a 23% Mg sample.

Coincidentally, in preliminary tests conducted before our reduced gravity flights, it was found that *loose* powder mixtures with JSC-1A milled for 4 hours (< 70 μm) also featured spin combustion. Pellets with the same mixture consistently burned without any sign of unsteady phenomena, indicating that compression of these mixtures has a significant effect on combustion stability.

Experiments with PBM JSC-1A behaved very differently. For these experiments, small amounts of mixture (approximately 3 g) were pressed to minimize the friction on the punch and die. Pressed samples showed reliable, steady combustion down to 13% Mg, which was determined experimentally to be the lower limit for reliable combustion. To our knowledge, this is the lowest metal concentration that has been achieved for SHS reactions involving JSC-1A. However, the reaction rate is quite low as a result (about 1 mm/s).

These findings are summarized in Figure 3.4g, which shows results for varying mixture ratios up to 26% Mg using simulant milled 2 h and simulant milled by PBM.

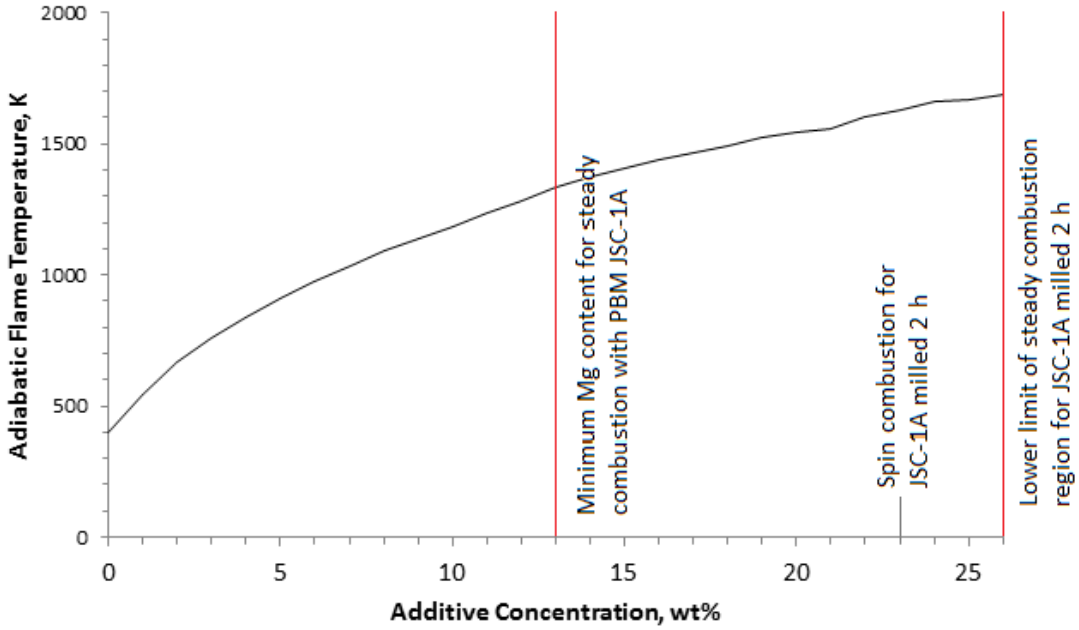

Figure 3.4g: Expansion of the steady combustion region due to milling.

What is clear from the results is that milling the simulant with a planetary ball mill resulted in a significant expansion of the steady combustion region. This is likely due to a number of factors, including the increase in surface area, the reduction in relative density (which, in turn, reduces the thermal diffusivity), and compression of the mixture, which increases the contact between particles.

4. Conclusion

Thermodynamic calculations of the adiabatic flame temperature and combustion products were conducted for the mixtures of Al and Mg with JSC-1A lunar regolith simulant over the range of metal concentrations from 0 to 100 wt%. The combustion product compositions of Al-based mixtures accord well with prior experimental data. At the same metal concentrations, the calculations predict higher adiabatic flame temperatures for Mg-based mixtures. The maximum temperatures are reached at 23 wt% Al and 26 wt% Mg.

Combustion of Mg/JSC-1A mixture pellets in argon environment was studied experimentally. Prior to mixing with Mg, the used JSC-1A powder was ball-milled. At the volume weighted mean diameter less than 100 μm, ignition and stable propagation of the combustion front was observed in all experiments. It was shown that with increasing the milling time of JSC-1A, the combustion front velocity of Mg/JSC-1A mixture increases. A decrease in argon pressure from 90 kpa to 10 kPa does not influence the front velocity.

The effect of gravity on product composition was studied experimentally and was found to affect concentrations of the mineral products. The number of products does not appear to vary, and the quantitative results show good agreement with calculations. Experiments to minimize the amount of magnesium determined 13% Mg to be the lower limit of stable, reliable combustion when the simulant had been milled in a planetary ball mill.

References

Entries have been arranged by category (books, journal articles, reports, theses/dissertations, presentations and conference papers, websites). Within each category the ordering is alphabetical by last name.

Books

Boles, Michael A., and Yunus A. Çengel. *Thermodynamics: An Engineering Approach*, 6th ed. New York: McGraw-Hill, 2008.

Cadogan, Peter H. *The Moon – Our Sister Planet*. New York: Cambridge University Press, 1981.

Callister Jr., William D. *Fundamentals of Materials Science and Engineering*, 5th ed. New York: John Wiley & Sons, 2001.

Frankhouser, William L. *Advanced Processing of Ceramic Compounds: Dynamic Compaction Technology, Self-Propagating High-Temperature Synthesis, Plasmachemical Technology*. Park Ridge, NJ: Noyes Data Corporation, 1987.

Guerrieri, Mary L., John S. Lewis, and Mildred Shapely Matthews, eds. *Resources of Near-Earth Space*. Tucson: University of Arizona Press, 1993.

Lunar and Planetary Institute. *Lunar Sourcebook: A User's Guide to the Moon*. New York: Cambridge University Press, 1991.

Mendell, W. W., ed. *Lunar Bases and Space Activities of the 21st Century*. Houston: Lunar and Planetary Institute, 1985.

Saxena, Surendra. "Systematization and Estimation of Thermochemical Data on Silicates." In *Modelling in Aquatic Chemistry*, by Ingmar Grenthe and Ignasi Puigdomenech, 289-323. OECD Publications, 1997.

Articles

Agui, Juan, Vivake Asnani, Chunmei He, Heather Oravec, Allen Wilkinson, and Xiangwu Zeng. "Geotechnical Properties of JSC-1A Lunar Soil Simulant." *Journal of Aerospace Engineering* 23, no. 2 (April 2010): 111-116.

Alshibli, Khalid A., and Alsidqi Hasan. "Strength Properties of JSC-1A Lunar Regolith Simulant." *Journal of Geotechnical and Geoenvironmental Engineering* 135 no. 5 (May 2009): 673-679.

Arslan, Haydar, Susan Batiste, and Stein Sture. "Engineering Properties of Lunar Soil Simulant JSC-1A." *Journal of Aerospace Engineering* 23, no. 1 (January 2010): 70-83.

Aruna, Singanahally T., Sambandan Ekambaram, and Kashinath C. Patil. “Combustion Synthesis.” *Current Opinion in Solid State and Materials Science* 2 (1997): 158-165.

Balasubramaniam R., Gokoglu S., Sacksteder K., Wegeng R., and Suzuki N., “Analysis of Solar-Heated Thermal Wadis to Support Extended-Duration Lunar Exploration*.” Journal of Thermophysics and Heat Transfer* 25 no. 1 (2011): 130-139.

Barraclough, B. L., A. B. Binder, R. C. Elphic, W. C. Feldman, D. J. Lawrence, and P. G. Lucey. “Lunar Fe and Ti Abundances: Comparison of Lunar Prospector and Clementine Data.” *Science* 281 no. 4 (September 1998): 1493-1496.

Borovinskaya, I. P., A. K. Filonenko, A. G. Merzhanov, and N. P. Novikov. “Gasless Combustion of Mixtures of Powdered Transition Metals with Boron.” *Combustion, Explosion, and Shock Waves* 10 no. 1 (1974): 4-15.

Borovinskaya, I. P., and A. G. Merzhanov. “Self-Propagated High-Temperature Synthesis of Refractory Inorganic Compounds.” *Doklady Akademii Nauk SSSR* 204 no. 2 (May 1972): 366-369.

Cocks, Alan C. F. “Constitutive Modelling of Powder Compaction and Sintering.” *Progress in Materials Science* 46 (2001): 201-229.

Campos, José, Antonio Correia, Benilde F. O. Costa, Luisa Durães, António Portugal, and Regina Santos. “Fe_2O_3/Aluminum Thermite Reaction Intermediate and Final Products Characterization.” *Materials Science and Engineering A* 465 (2007): 199-210.

Campos, José, Luísa Durães, and António Portugal. “Radial Combustion Propagation in Iron(III) Oxide/Aluminum Thermite Mixtures.” *Propellants, Explosives, Pyrotechnics* 31 no. 1 (2006): 42-49.

Deane, Bill, Eddy Hill, Yang Liu, Michael J. Mellin, and Lawrence A. Taylor. “Apollo Sample 70051 and High- and Low-Ti Lunar Soil Simulants MLS-1A and JSC-1A: Implications for Future Lunar Exploration.” *Journal of Geophysical Research* 112 (2007).

Dimaki, A. V., S. G. Psakh’e, and E. V. Shil’ko. “Simulating the Propagation of Exothermic Reactions in Heterogeneous Media.” *Combustion, Explosion, and Shock Waves* 41 no. 2 (2005): 151-157.

Drozdova, I. A., A. E. Lapshin, and L. V. Morozova. “Preparation and Investigation of Porous Aluminosilicate Ceramic Materials.” *Glass Physics and Chemistry* 34 no. 4 (2008): 443-448.

Dvoryankin, A. V., A. G. Merzhanov, and A. G. Strunina. “Stability of Combustion in Thermite Systems.” *Combustion, Explosion, and Shock Waves* 21 no. 4 (1985): 421-425.

------. “Unstable Regimes of Thermite System Combustion.” *Combustion, Explosion, and Shock Waves* 19 no. 2 (1983): 158-163.

Feng, H. J., and John J. Moore. “Combustion Synthesis of Advanced Materials: Part I. Reaction Parameters.” *Progress in Materials Science* 39 (1995): 243-273.

------. “Combustion Synthesis of Advanced Materials: Part II. Classification, Applications and Modelling.” *Progress in Materials Science* 39 (1995): 275-316.

Garboczi, E. J. “Three Dimensional Shape Analysis of JSC-1A Simulated Lunar Regolith Particles.” Powder Technology 207 (February 2011): 96-103.

Heiken, Grant. “Petrology of Lunar Soils.” *Reviews of Geophysics and Space Physics* 13 no. 4 (August 1975): 567-587.

Hanson, G. N. and C. H. Langmuir. “Calculating Mineral-Melt Equilibria with Stoichiometry, Mass Balance, and Single-Component Distribution Coefficients.” *Advances in Physical Geochemistry* 1 (1981). Reprint from *Thermodynamics of Minerals and Melts*.

Ivleva, T. P., and A. G. Merzhanov. “Three-Dimensional Spinning Waves in the Case of Gas-Free Combustion.” *Doklady Physics* 45 no. 4 (2000): 136-141.

Kaydash, V. G., C. M. Pieters, and Yu G. Shkuratov. “Lunar Clinopyroxene and Plagioclase: Surface Distribution and Composition.” *Solar System Research* 39 no. 4 (2005): 255-266.

Lau, Cheryl, and Alexander Mukasyan. “Influence of Gravity on Combustion Synthesis of Advanced Materials.” *AIAA Journal* 43 no. 2 (February 2005).

Lau, Cheryl, Alexander S. Mukasyan, and Arvind Varma. “Materials Synthesis by Reduction-Type Combustion Reactions: Influence of Gravity.” *Proceedings of the Combustion Institute* 29 (2002): 1101-1108.

Leuenberger, Hans, and Bhagwan Dass Rohera. “Fundamentals of Powder Compression. I. The Compactibility and Compressibility of Pharmaceutical Powders.” *Pharmaceutical Research* 3 no. 1 (1986): 12-22.

Makino, Atsushi. “Initiation of SHS Flame Induced by Another SHS Flame---Evaluation of the Ignition Energy.*” Journal of Energy Resources Technology* 123 (March 2001): 70-75.

------. “Effects of Heat Loss on the SHS Flame Propagation.” *Energy Conversion and Management* 38 no. 10-13 (1997): 1043-1049.

------. “Heterogeneous Flame Propagation in the Self-Propagating, High-Temperature, Synthesis (SHS) Process in Multi-Layer Foils: Theory and Experimental Comparisons.” *Combustion and Flame* 134 (2003): 273-288.

Maksimov, E. I., Merzhanov, A. G., and Shkiro, V. M. “Gasless Compositions as a Simple Model for the Combustion of Nonvolatile Condensed Systems.” *Combustion, Explosion, and Shock Waves* 1 no. 4 (1965): 15-18.

Meek, T. T., and L. A. Taylor. “Microwave Sintering of Lunar Soil: Properties, Theory, and Practice,” Journal of Aerospace Engineering 18 no. 3 (2005): 188–196.

Merzhanov, Alexander. “The Chemistry of Self-Propagating High-Temperature Synthesis.” *Journal of Materials Chemistry* 14 (2004): 1779-1786.

Mossino, P. “Some Aspects in Self-Propagating High-Temperature Synthesis.” *Ceramics International* 30 (2004): 311-332.

Mukasyan, Alexander S., and Arvind Varma. “Combustion Synthesis of Advanced Materials: Fundamentals and Applications.” *Korean Journal of Chemical Engineering* 21, no. 2 (2004): 527-536.

O’Dell, J. S., C. S. Ray, S. T. Reis, and S. Sen. “JSC-1A Lunar Soil Simulant: Characterization, Glass Formation, and Selected Glass Properties.” *Journal of Non-Crystalline Solids* 356 (2010): 2369-2374.

Shafirovich, E., Diakov, V., and Varma, A., “Combustion-Assisted Hydrolysis of Sodium Borohydride for Hydrogen Generation,” *International Journal of Hydrogen Energy* 32 no. 2 (2007): 207-211.

Shiryaev, A. A., “Thermodynamics of SHS Processes: Advanced Approach,” *International Journal of Self-Propagating High-Temperature Synthesis* 4 no. 4 (1995): 351-362.

Simonsen, L. C., Nealy, J. E., Townsend, L. W., Wilson, J. W., “Martian Regolith as Space Radiation Shielding.” *Journal of Spacecraft and Rockets* 28 no.1 (1991): 7-8.

Sinka, I. C. “Modelling Powder Compaction.” *KONA* (Hosokawa Powder Technology Foundation, Japan) 25 (2007): 4-22.

Wänke, Heinrich. “Chemistry of the Moon.” *Topics in Current Chemistry* 44 (1974): 115-154.

Reports

Lunar and Planetary Institute. “Workshop on Using In Situ Resources for Construction of Planetary Outposts,” edited by M. B. Duke. LPI Technical Report Number 98-01. Workshop sponsored by LPI, NASA, and Space ’98. Held in Albuquerque, NM, April 30 – May 1, 1998.

National Aeronautics and Space Administration. *Characterization Summary of JSC-1A Bulk Lunar Mare Regolith Simulant*. Version B.1. Marshall Space Flight Center, 2007.

------. *Characterization Summary of JSC-1AF Lunar Mare Regolith Simulant*. Version 1.6.2. Marshall Space Flight Center, 2006.

------. *Generation of Requirements for Simulant Measurements*, by Doug Rickman and Jennifer Edmunson. Marshall Space Flight Center, 2010.

------. *Grain Size Analysis of UTEP Samples*, by Bonnie L. Cooper and David S. McKay. Johnson Space Center, 2011.

------. *Handbook of Lunar Materials*. Johnson Space Center, 1980.

------. *Lunar Regolith Simulant User's Guide*, by C. M. Schrader, D. L. Rickman, C. A. McLemore, and J. C. Fikes. Marshall Space Flight Center, 2010.

------. *The Need for High Fidelity Lunar Regolith Simulants*, by James R. Gaier. Glenn Research Center, 2008.

Omar, Husam A. "Production of Lunar Concrete Using Molten Sulfur." Final research report for JoVe NASA grant NAG8-278. 2009.

Theses and Dissertations

Faierson, Eric J. 2009. Influences of Reaction Parameters on the Product of a Geothermite Reaction: A Multi-Component Oxidation-Reduction Reaction Study. Master's thesis. Virginia Polytechnic Institute and State University.

Masafumi Iai. 2010. Scaled experimental study on excavation of lunar regolith with rakes/rippers and flat blade. PhD diss., Missouri University of Science and Technology. In Scholars' Mine Research Repository, http://scholarsmine.mst.edu/thesis/Scaled_experimental__09007dcc80849963.html (accessed November 7, 2011).

Presentations

Botha, Pieter, Alan Butcher, John Fikes, Carole McLemore, Doug Rickman, Christian Schrader, Doug Stoeser, and Stephen Wilson. "Extant and Extinct Lunar Regolith Simulants: Modal Analyses of NU-LHT-1M and -2m, OB-1, JSC-1, JSC-1A and -1AF, FJS-1, and MLS-1." Presentation given at the Planetary & Terrestrial Mining Sciences Symposium. Montreal, Quebec, 2008.

Duke, Michael B. "Use of Combustion Synthesis for Parts Fabrication Using Lunar Materials." Paper presented at the Fourth International Conference on Exploration and Utilisation of the Moon: ICEUM 4. Held 10-14 July, 2000, at ESTEC, Noordwijk, The Netherlands.

Faierson, Eric J., and Kathryn V. Logan. "Geothermite Reactions for In-Situ Resource Utilization on the Moon and Beyond." Paper presented at the Earth & Space 2010 Conference, sponsored by the American Society of Civil Engineers, Honolulu, HI, March 14-17, 2010.

Faeirson, Eric J., et al. "Lunar Construction and Resource Extraction Utilizing Lunar Regolith." Paper presented at the 2008 Pacific International Space Center for Exploration Systems (PISCES) & Japan-U.S. Technology & Space Applications Program (JUSTSAP) Conference. November 2008.

Luss, D., and Martirosyan, K.S. "Combustion Synthesis of Ceramic Composites from Lunar Soil Simulant," *Lunar and Planetary Science Conference XXXVII*, League City, TX, 2006, Abstract # 1896, http://www.lpi.usra.edu/meetings/lpsc2006/pdf/1896.pdf [retrieved 21 February 2011].

Ray, Chandra, Doug Rickman, Daniel A. Scheiman, Kenneth W. Street Jr. "Thermal Properties of Lunar Regolith Simulants." Paper presented at the Earth & Space 2010 Conference, sponsored by the American Society of Civil Engineers, Honolulu, HI, March 14-17, 2010.

Yang Liu and Lawrence A. Taylor. “Important Considerations for Lunar Soil Simulants.” Paper presented at the Earth & Space 2010 Conference, sponsored by the American Society of Civil Engineers, Honolulu, HI, March 14-17, 2010.

Websites

Merzhanov, A. G., and A. E. Sytschev. “About Self-Propagating High-Temperature Synthesis.” Institute of Structural Macrokinetics and Materials Science, Russian Academy of Sciences. http://www.ism.ac.ru/handbook/_shs.htm (accessed January 1, 2010).

Appendix

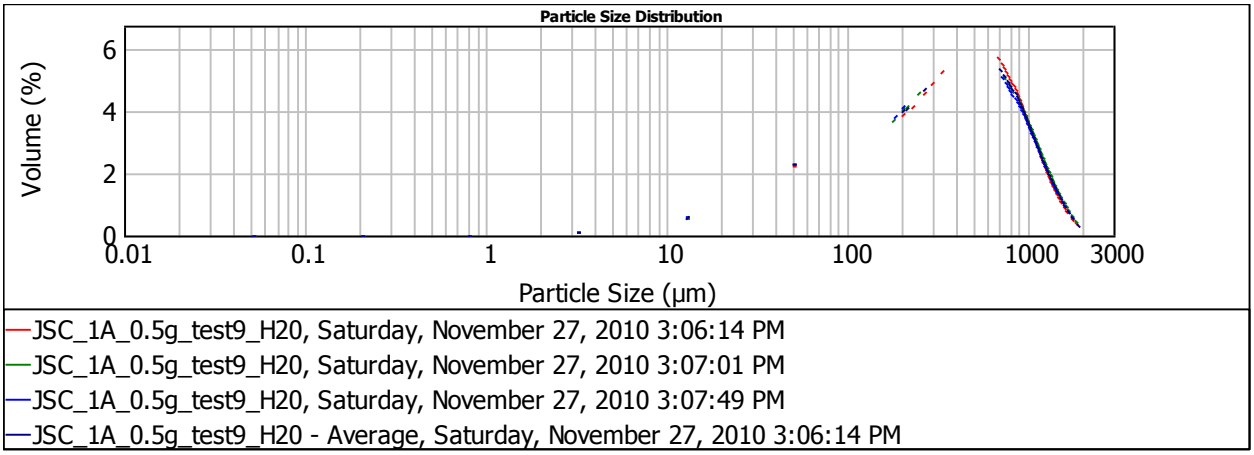

D [4, 3] - Volume weighted mean	Uniformity	Specific surface area	D [3, 2] - Surface weighted mean	d (0.1)	d (0.5)	d (0.9)
397.166	0.905	0.0647	92.773	37.044	303.261	901.166
397.596	0.952	0.0657	91.291	36.476	292.229	923.402
387.393	0.969	0.0683	87.883	34.964	282.13	902.673
394.052	0.942	0.0662	90.602	36.136	292.403	908.941

Figure A1: Size distribution of JSC-1A measured with water.

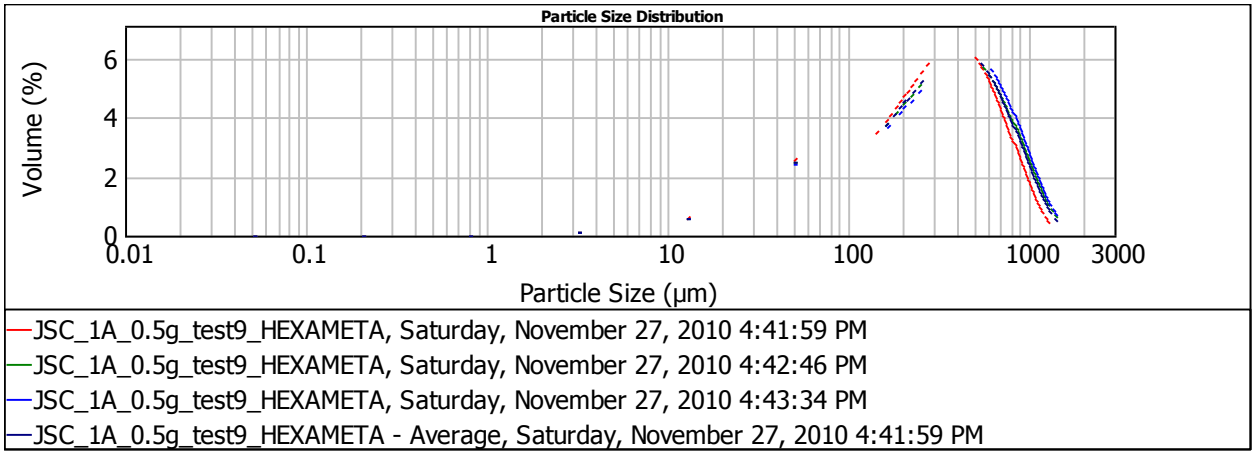

D [4, 3] - Volume weighted mean	Uniformity	Specific surface area	D [3, 2] - Surface weighted mean	d (0.1)	d (0.5)	d (0.9)
304.885	0.842	0.0721	83.199	34.248	242.023	678.247
336.955	0.895	0.0696	86.179	35.178	256.87	763.479
349.62	0.89	0.0684	87.696	35.604	268.414	789.45
330.486	0.879	0.0701	85.65	34.994	255.179	743.738

Figure A2: Size distribution of JSC-1A measured with L-1 sodium hexametaphosphate.

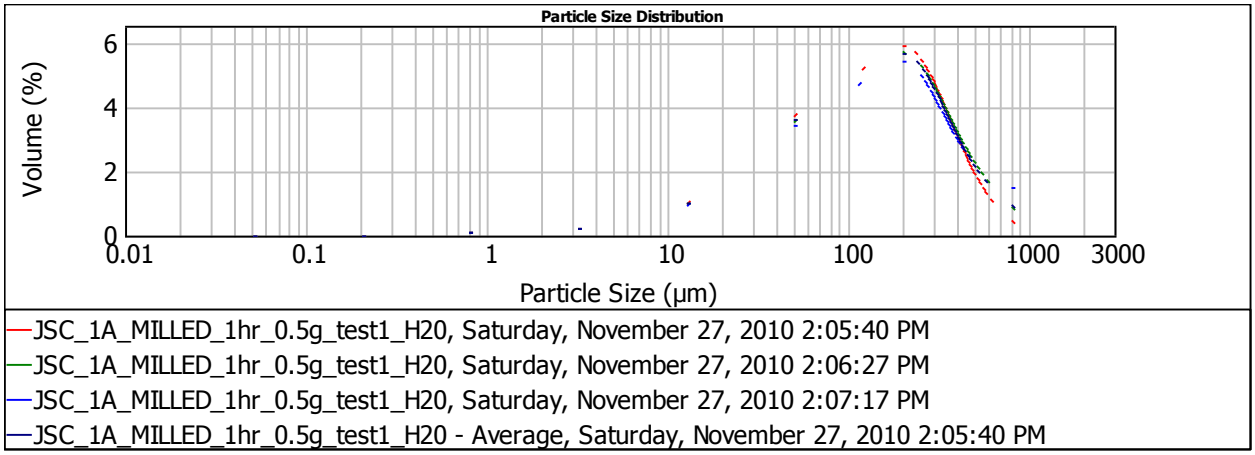

D [4, 3] - Volume weighted mean	Uniformity	Specific surface area	D [3, 2] - Surface weighted mean	d (0.1)	d (0.5)	d (0.9)
160.445	0.94	0.188	31.937	21.006	115.922	360.21
177.906	1.02	0.184	32.688	21.319	121.745	406.81
214.338	1.24	0.179	33.455	21.635	128.506	513.44
184.23	1.07	0.184	32.681	21.318	121.854	414.9

Figure A3: Size distribution of JSC-1A milled for 1 h, measured with water.

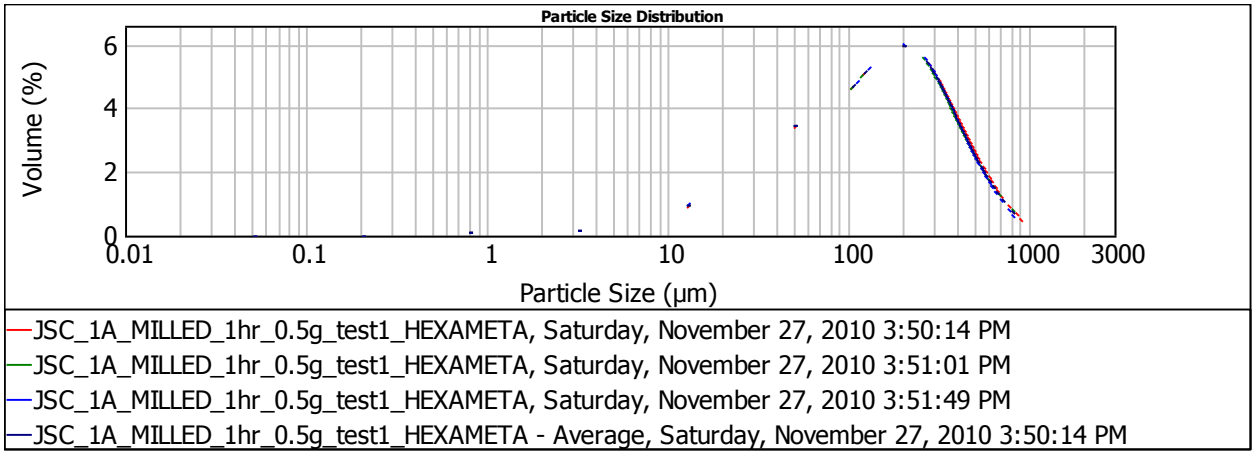

D [4, 3] - Volume weighted mean	Uniformity	Specific surface area	D [3, 2] - Surface weighted mean	d (0.1)	d (0.5)	d (0.9)
181.472	0.941	0.161	37.275	22.97	131.276	413.625
181.423	0.963	0.165	36.383	22.416	129.318	410.881
177.161	0.942	0.168	35.813	22.058	128.445	401.485
180.019	0.949	0.164	36.481	22.476	129.677	408.581

Figure A4: Size distribution of JSC-1A milled for 1 h, measured with L-1 sodium hexametaphosphate.

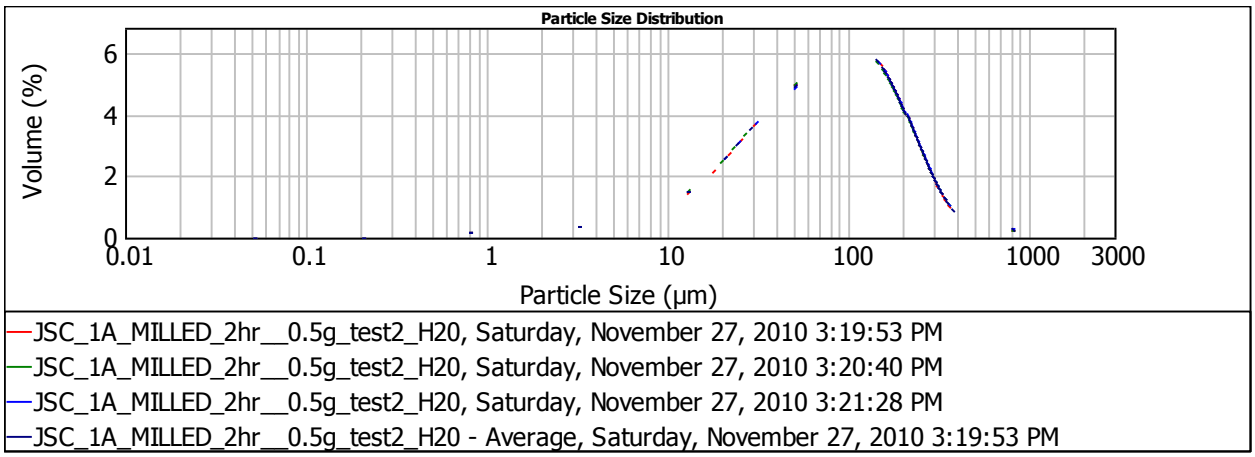

D [4, 3] - Volume weighted mean	Uniformity	Specific surface area	D [3, 2] - Surface weighted mean	d (0.1)	d (0.5)	d (0.9)
106.32	0.968	0.292	20.514	14.632	73.899	220.339
104.824	0.967	0.297	20.189	14.342	73.027	221.334
108.281	0.994	0.295	20.318	14.4	74.133	224.564
106.475	0.976	0.295	20.339	14.457	73.684	222.056

Figure A5: Size distribution of JSC-1A milled for 2 h, measured with water.

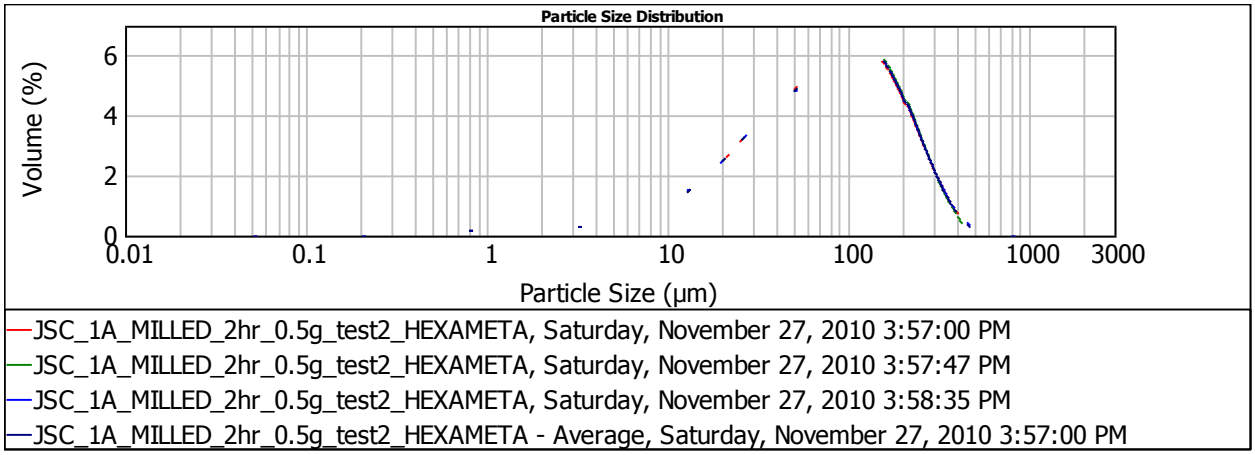

D [4, 3] - Volume weighted mean	Uniformity	Specific surface area	D [3, 2] - Surface weighted mean	d (0.1)	d (0.5)	d (0.9)
98.246	0.848	0.287	20.901	14.71	74.558	216.103
97.867	0.835	0.287	20.879	14.652	75.196	214.706
98.735	0.848	0.289	20.752	14.512	75.181	216.994
98.283	0.844	0.288	20.844	14.625	74.976	215.925

Figure A6: Size distribution of JSC-1A milled for 2 h, measured with L-1 sodium hexametaphosphate.

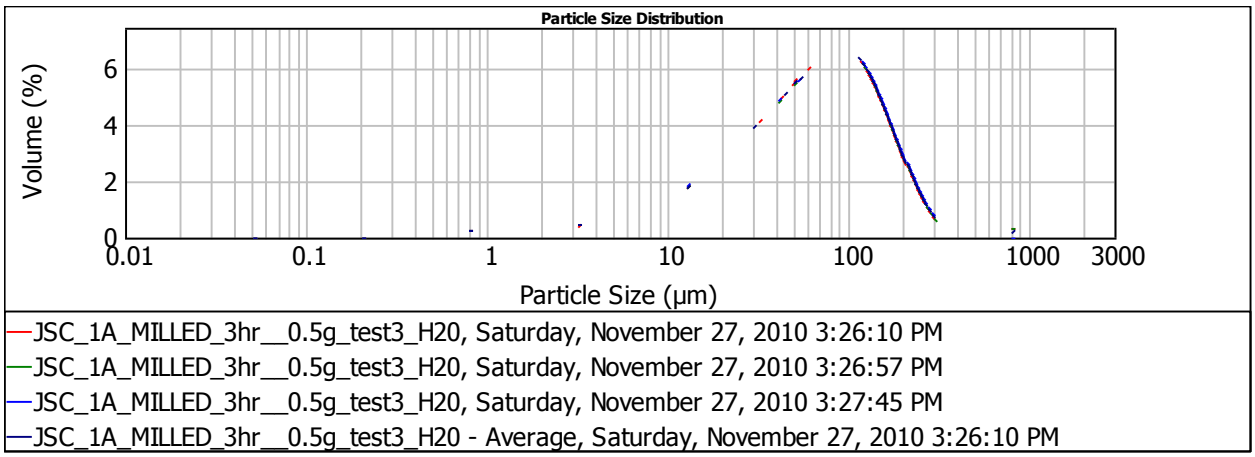

D [4, 3] - Volume weighted mean	Uniformity	Specific surface area	D [3, 2] - Surface weighted mean	d (0.1)	d (0.5)	d (0.9)
92.947	1.02	0.366	16.394	11.514	62.441	172.038
95.299	1.05	0.367	16.334	11.428	62.694	173.723
77.276	0.792	0.374	16.03	11.186	61.364	165.776
88.507	0.956	0.369	16.251	11.375	62.163	170.385

Figure A7: Size distribution of JSC-1A milled for 3 h, measured with water.

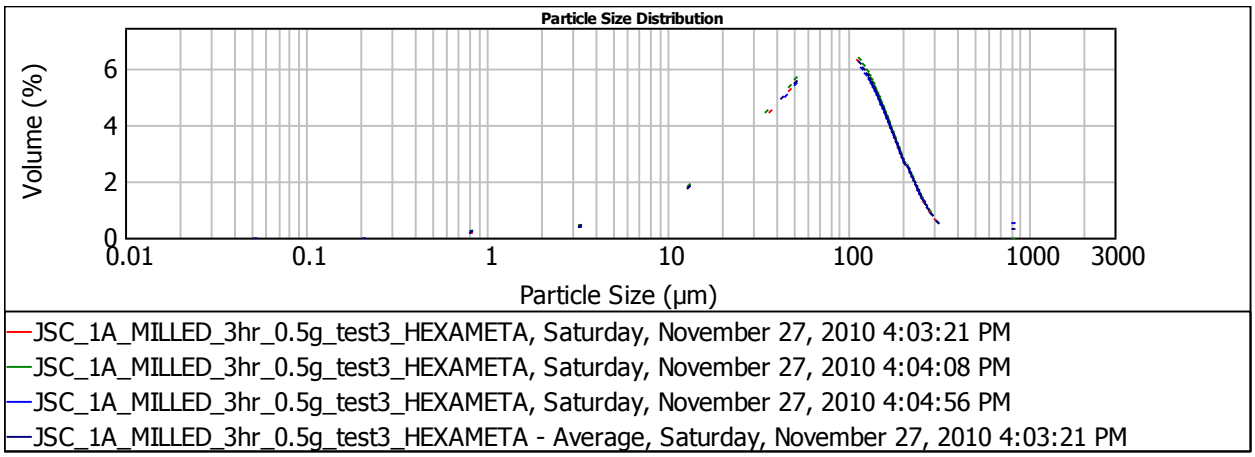

D [4, 3] - Volume weighted mean	Uniformity	Specific surface area	D [3, 2] - Surface weighted mean	d (0.1)	d (0.5)	d (0.9)
105.966	1.2	0.356	16.877	11.834	63.39	181.046
75.929	0.787	0.372	16.135	11.246	60.405	162.799
107.843	1.24	0.361	16.637	11.598	63.01	184.341
96.579	1.08	0.363	16.544	11.555	62.241	175.192

Figure A8: Size distribution of JSC-1A milled for 3 h, measured with L-1 sodium hexametaphosphate.

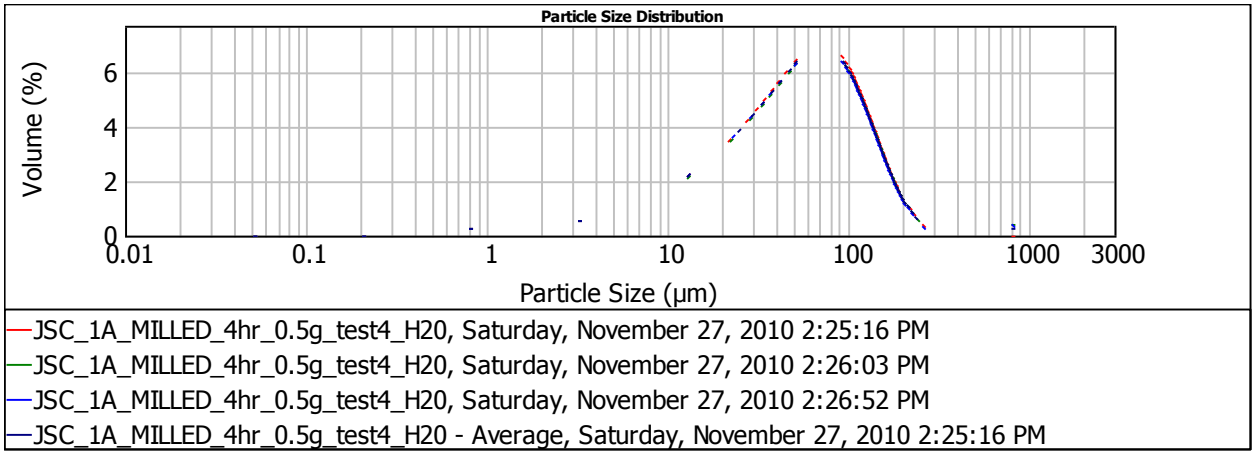

D [4, 3] - Volume weighted mean	Uniformity	Specific surface area	D [3, 2] - Surface weighted mean	d (0.1)	d (0.5)	d (0.9)
61.082	0.757	0.455	13.174	8.71	49.741	129.291
82.582	1.15	0.446	13.454	8.902	51.138	140.073
75.104	1.04	0.456	13.154	8.643	49.939	135.773
72.923	0.981	0.453	13.259	8.751	50.267	134.779

Figure A9: Size distribution of JSC-1A milled for 4 h, measured with water.

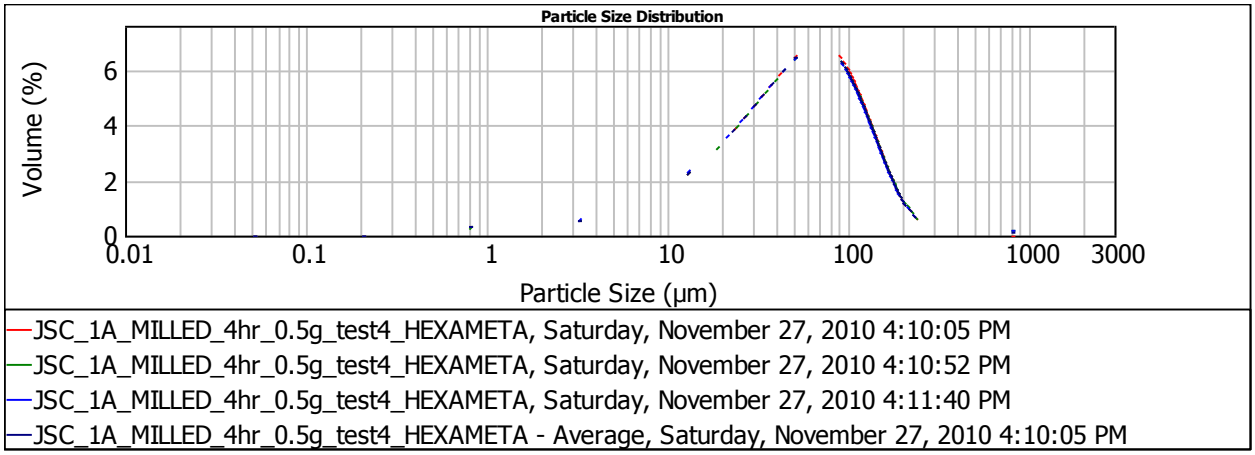

D [4, 3] - Volume weighted mean	Uniformity	Specific surface area	D [3, 2] - Surface weighted mean	d (0.1)	d (0.5)	d (0.9)
59.356	0.765	0.467	12.844	8.421	47.991	126.353
65.123	0.88	0.466	12.884	8.432	48.217	130.091
63.498	0.867	0.473	12.697	8.259	47.511	128.598
62.659	0.837	0.468	12.808	8.371	47.906	128.306

Figure A10: Size distribution of JSC-1A milled for 4 h, measured with L-1 sodium hexametaphosphate.

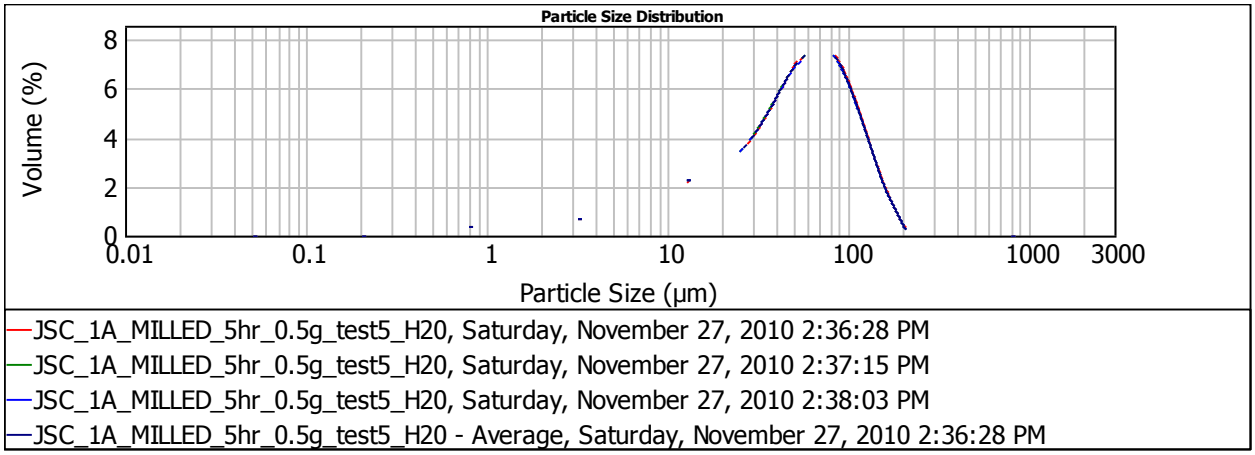

D [4, 3] - Volume weighted mean	Uniformity	Specific surface area	D [3, 2] - Surface weighted mean	d (0.1)	d (0.5)	d (0.9)
55.381	0.695	0.528	11.365	6.612	48.336	114.414
54.815	0.702	0.535	11.216	6.482	47.642	113.643
54.692	0.704	0.538	11.151	6.422	47.515	113.542
54.963	0.7	0.534	11.243	6.505	47.833	113.869

Figure A11: Size distribution of JSC-1A milled for 5 h, measured with water.

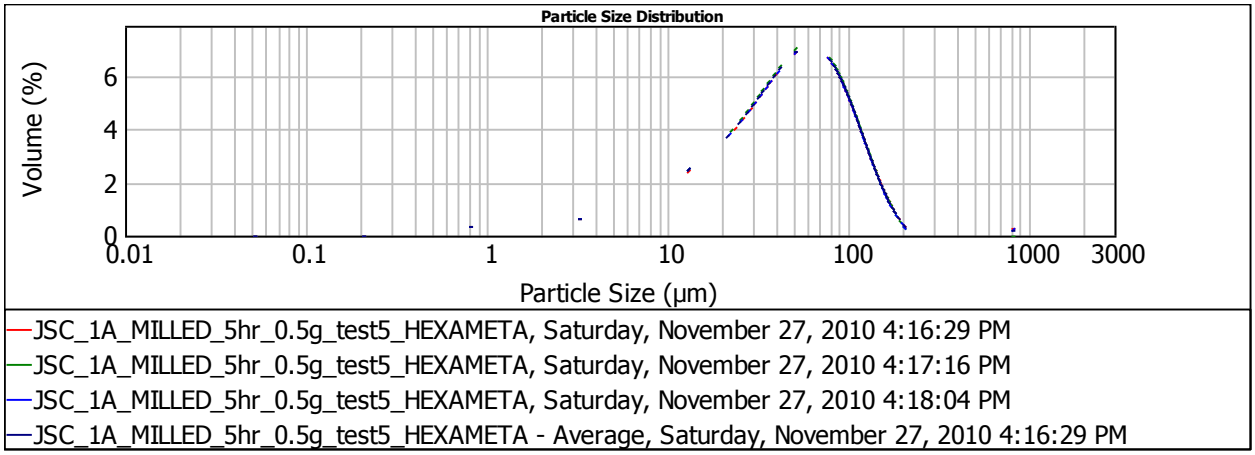

D [4, 3] - Volume weighted mean	Uniformity	Specific surface area	D [3, 2] - Surface weighted mean	d (0.1)	d (0.5)	d (0.9)
70.676	1.15	0.519	11.555	7.182	43.632	114.308
50.949	0.735	0.533	11.255	6.94	42.366	107.135
67.111	1.09	0.526	11.41	7.046	43.175	112.649
62.912	0.994	0.526	11.406	7.055	43.052	111.235

Figure A12: Size distribution of JSC-1A milled for 5 h, measured with L-1 sodium hexametaphosphate.

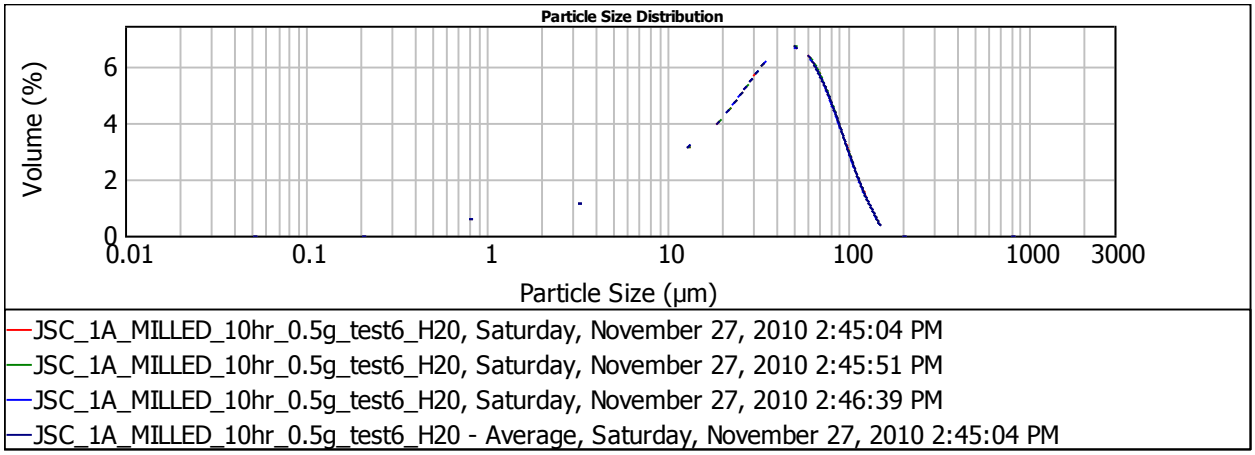

D [4, 3] - Volume weighted mean	Uniformity	Specific surface area	D [3, 2] - Surface weighted mean	d (0.1)	d (0.5)	d (0.9)
36.77	0.806	0.84	7.142	3.377	29.88	80.419
36.721	0.804	0.841	7.138	3.375	29.892	80.254
36.466	0.809	0.847	7.084	3.331	29.578	79.889
36.652	0.806	0.843	7.121	3.361	29.783	80.188

Figure A13: Size distribution of JSC-1A milled for 10 h, measured with water.

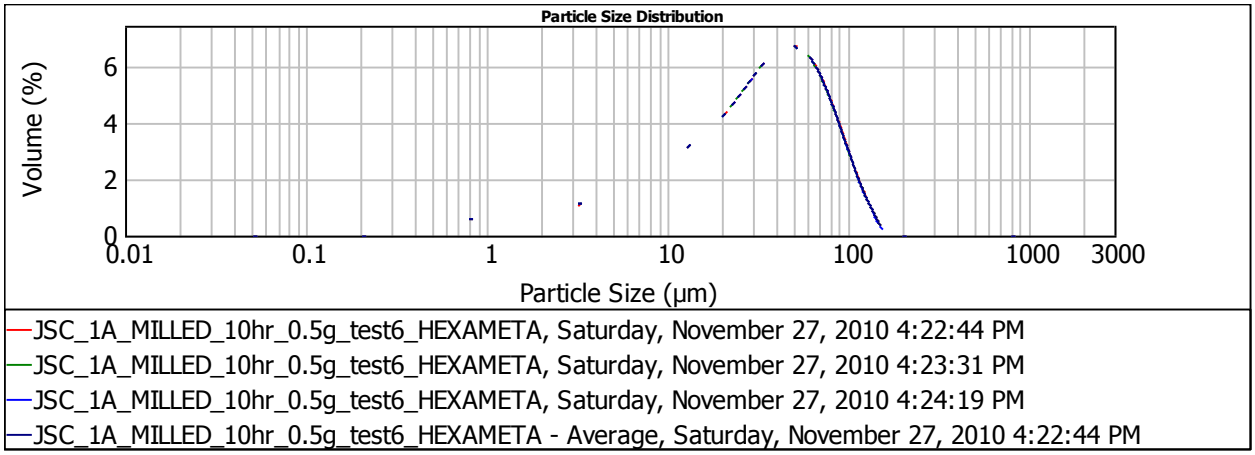

D [4, 3] - Volume weighted mean	Uniformity	Specific surface area	D [3, 2] - Surface weighted mean	d (0.1)	d (0.5)	d (0.9)
36.824	0.803	0.83	7.232	3.436	29.946	80.446
36.654	0.806	0.833	7.2	3.41	29.761	80.141
36.608	0.805	0.835	7.189	3.399	29.747	80.07
36.695	0.805	0.833	7.207	3.415	29.818	80.22

Figure A14: Size distribution of JSC-1A milled for 10 h, measured with L-1 sodium hexametaphosphate.

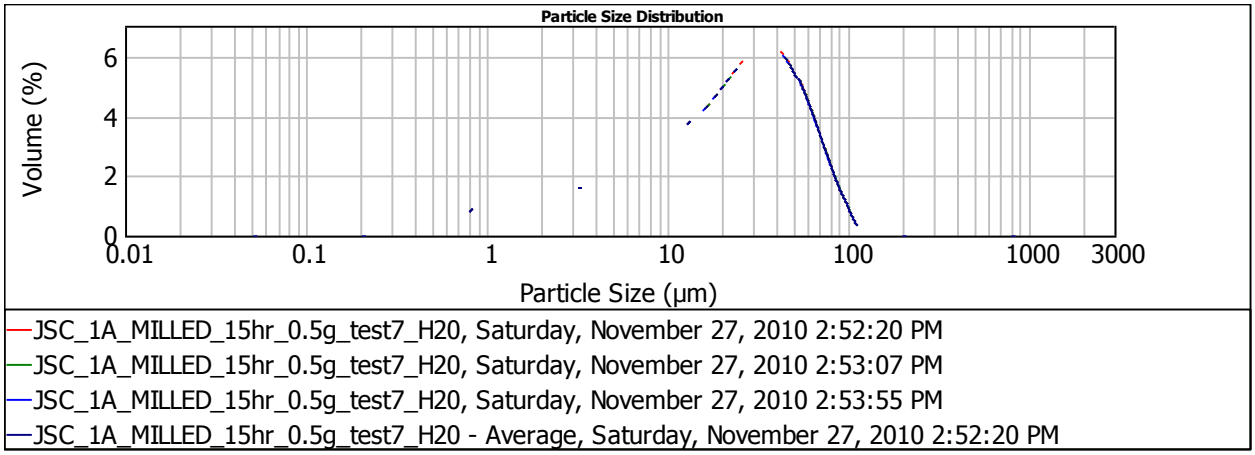

D [4, 3] - Volume weighted mean	Uniformity	Specific surface area	D [3, 2] - Surface weighted mean	d (0.1)	d (0.5)	d (0.9)
26.12	0.864	1.15	5.205	2.068	20.621	58.64
26.108	0.869	1.16	5.19	2.059	20.528	58.728
25.975	0.869	1.16	5.171	2.049	20.412	58.465
26.068	0.867	1.16	5.189	2.059	20.52	58.611

Figure A15: Size distribution of JSC-1A milled for 15 h, measured with water.

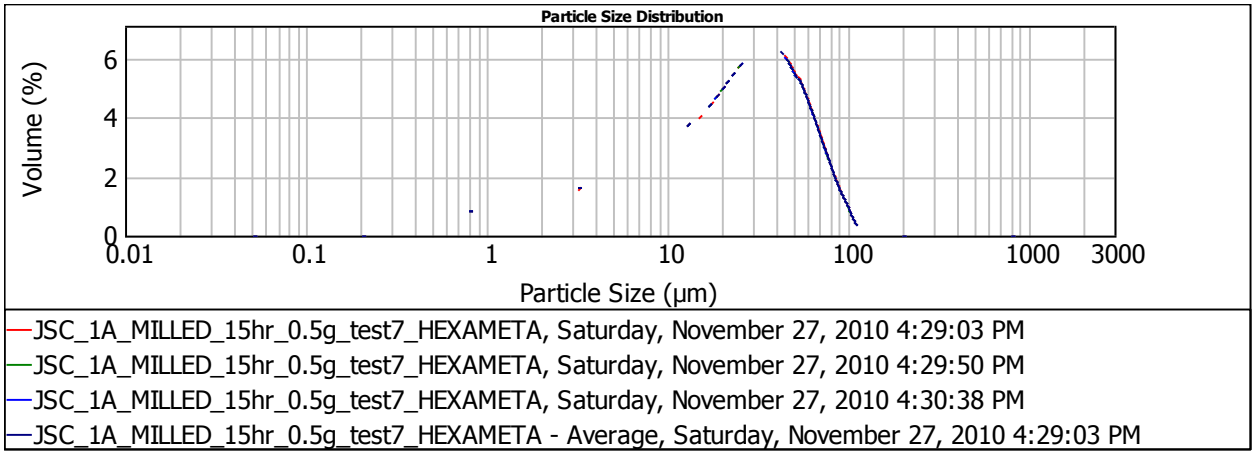

D [4, 3] - Volume weighted mean	Uniformity	Specific surface area	D [3, 2] - Surface weighted mean	d (0.1)	d (0.5)	d (0.9)
26.4	0.856	1.14	5.274	2.101	20.975	59.061
26.282	0.858	1.14	5.252	2.088	20.839	58.852
26.285	0.861	1.14	5.251	2.087	20.804	58.916
26.322	0.858	1.14	5.259	2.092	20.872	58.943

Figure A16: Size distribution of JSC-1A milled for 15 h, measured with L-1 sodium hexametaphosphate.

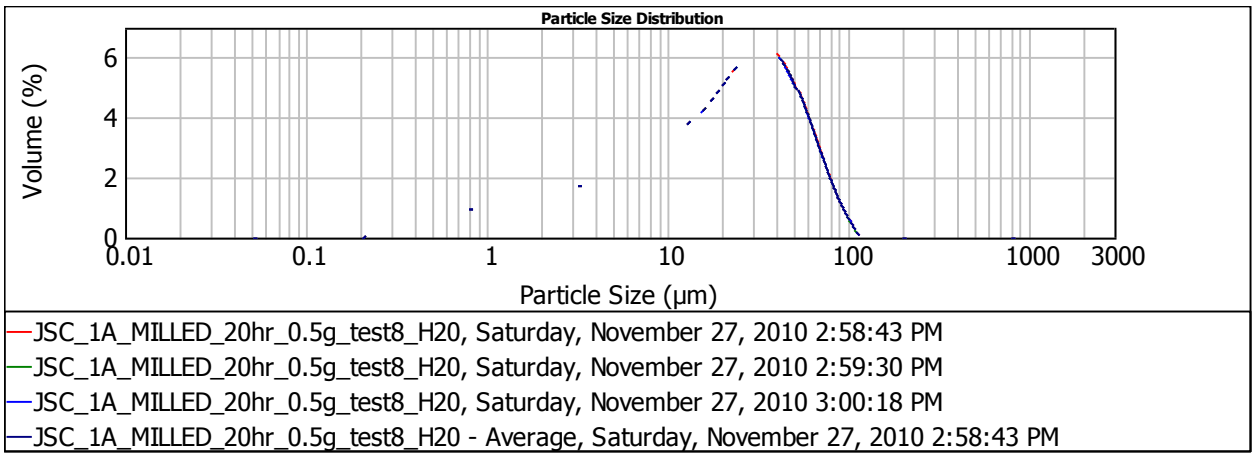

D [4, 3] - Volume weighted mean	Uniformity	Specific surface area	D [3, 2] - Surface weighted mean	d (0.1)	d (0.5)	d (0.9)
24.503	0.878	1.26	4.757	1.817	19.254	55.379
24.39	0.883	1.27	4.736	1.806	19.104	55.212
24.357	0.885	1.27	4.727	1.801	19.05	55.182
24.417	0.882	1.27	4.74	1.808	19.136	55.258

Figure A17: Size distribution of JSC-1A milled for 20 h, measured with water.

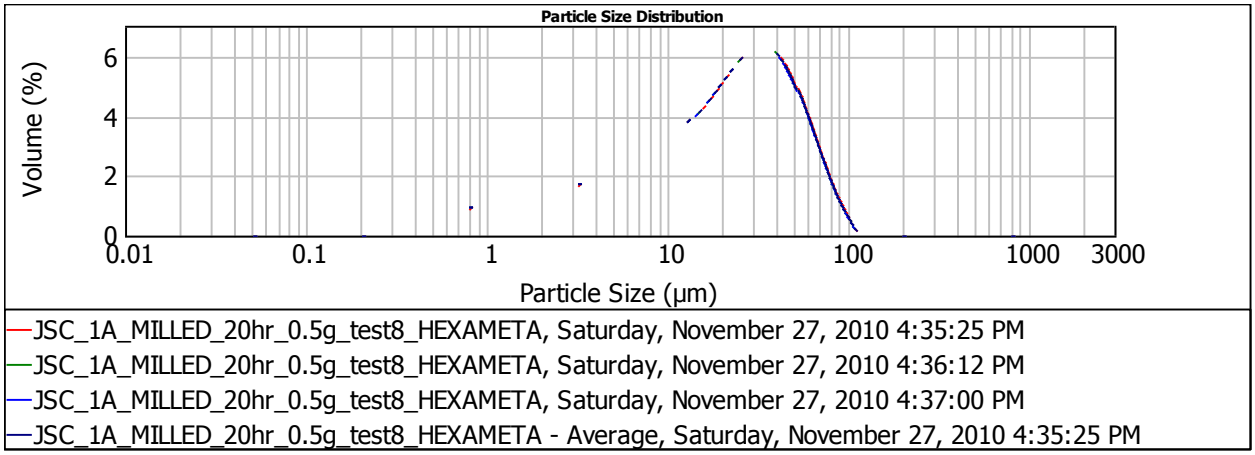

D [4, 3] - Volume weighted mean	Uniformity	Specific surface area	D [3, 2] - Surface weighted mean	d (0.1)	d (0.5)	d (0.9)
24.572	0.866	1.22	4.918	1.891	19.428	55.246
24.326	0.871	1.23	4.882	1.872	19.171	54.777
24.25	0.873	1.23	4.866	1.864	19.079	54.653
24.382	0.87	1.23	4.888	1.876	19.226	54.893

Figure A18: Size distribution of JSC-1A milled for 20 h, measured with L-1 sodium hexametaphosphate.

Figure A19: Size distribution of UTEP's JSC-1A measured by Dr. Bonnie Cooper; Test 1.

Figure A20: Size distribution of UTEP's JSC-1A measured by Dr. Bonnie Cooper; Test 2.

Figure A21: Size distribution of UTEP's JSC-1A measured by Dr. Bonnie Cooper; Test 3.

Figure A22: Size distribution of JSC-1A milled by PBM, measured by Dr. Bonnie Cooper; Test 1.

Figure A22: Size distribution of JSC-1A milled by PBM, measured by Dr. Bonnie Cooper; Test 2.

Figure A23: Size distribution of JSC-1A milled by PBM, measured by Dr. Bonnie Cooper; Test 3.

Figure A24: Size distribution of PBM samples after sonication, measured by Dr. Bonnie Cooper; Test 1.

Figure A25: Size distribution of PBM samples after sonication, measured by Dr. Bonnie Cooper; Test 2.

Figure A26: Size distribution of PBM samples after sonication, measured by Dr. Bonnie Cooper; Test 3.

Vita

Christopher White was born in El Paso, Texas in 1986. He graduated from Canutillo High School and began his engineering studies at the University of Texas at El Paso (UTEP), finally earning the degree of Bachelor of Science in Mechanical Engineering in December of 2009. That year, he began working at UTEP's Center for Space Exploration and Technology Research, where he began his thesis studies in the field of in-situ resource utilization.

Permanent address: 128 Lisa Dr.
Canutillo, TX 79835

This thesis/dissertation was typed by the author.